

NACA RM A52D21

NACA

RESEARCH MEMORANDUM

TRANSONIC AERODYNAMIC CHARACTERISTICS OF THREE THIN
TRIANGULAR WINGS AND A TRAPEZOIDAL WING,
ALL OF LOW ASPECT RATIO

By Horace F. Emerson and Bernard M. Gale

Ames Aeronautical Laboratory
Moffett Field, Calif.

CLASSIFICATION CHANGED

To UNCLASSIFIED

By authority of *NACA Res. Lab. Effective*
** RN-114* Date *4-8-57*
NB 4-30-57

CLASSIFIED DOCUMENT

This material contains information affecting the National Defense of the United States within the meaning of the espionage laws, Title 18, U.S.C., Section 793 and 794; the transmission or revelation of which in any manner to an unauthorized person is prohibited by law.

NATIONAL ADVISORY COMMITTEE
FOR AERONAUTICS

WASHINGTON

July 18, 1952

CONFIDENTIAL

NACA LIBRARY
LANGLEY AERONAUTICAL LABORATORY
Langley Field, Va.



NATIONAL ADVISORY COMMITTEE FOR AERONAUTICS

RESEARCH MEMORANDUMTRANSONIC AERODYNAMIC CHARACTERISTICS OF THREE THIN
TRIANGULAR WINGS AND A TRAPEZOIDAL WING,
ALL OF LOW ASPECT RATIO

By Horace F. Emerson and Bernard M. Gale

SUMMARY


An investigation was conducted in the Ames 16-foot high-speed wind tunnel to determine the aerodynamic characteristics of three triangular wings and a trapezoidal wing through the transonic speed range, by use of the bump technique. Data were obtained throughout a Mach number range from 0.60 to 1.10 and a Reynolds number range from 2.1 million to 2.8 million.

Results of tests of the following wings are reported herein: Two aspect ratio 2 triangular wings having the NACA 0003-63 and 0005-63 sections, respectively, an aspect ratio 3 triangular wing having the NACA 0003-63 section, and a trapezoidal wing of aspect ratio 2 having the NACA 0003-63 section. The trapezoidal wing was obtained by cutting off the tips of the aspect ratio 3 triangular wing.

Lift, drag, and pitching-moment data are presented for all the wings investigated. Each of the wings, with the exception of the trapezoidal wing, had been previously tested in combination with a body in the Ames 6- by 6-foot supersonic wind tunnel and the results are presented herein as are data for the 5-percent-thick wing in combination with a body from tests conducted in the Ames 12-foot wind tunnel.

INTRODUCTION

The Ames Aeronautical Laboratory has in progress an experimental investigation of the aerodynamic characteristics of wings of interest in the design of high-speed fighter aircraft. This program included an investigation in the Ames 6- by 6-foot supersonic wind tunnel of two triangular wing-body combinations of aspect ratio 2, one with the



NACA 0005-63 section and the other with the NACA 0003-63 section, and one triangular wing-body combination of aspect ratio 3 with the NACA 0003-63 section. The Mach number range of these tests extended from 0.60 to 0.92 and from 1.2 to 1.7. An investigation of the aspect ratio 2 wing-body combination with the NACA 0005-63 section was also conducted in the Ames 12-foot pressure tunnel to obtain data from 0.24 to 0.95 Mach numbers. The models used in both of these investigations were full-span wing-body combinations that were sting supported. Further details may be found in references 1, 2, and 3.

In order to extend the Mach number range through the sonic speed, an investigation of similar wing models was undertaken on the transonic bump in the Ames 16-foot wind tunnel. In addition to the wings investigated in the 6- by 6-foot wind tunnel, the subject program included tests of a trapezoidal wing. The trapezoidal wing had an aspect ratio of 2 and was obtained by cutting the tip from the aspect ratio 3 triangular wing.

NOTATION

C_D	drag coefficient $\left(\frac{\text{twice semispan drag}}{qS} \right)$
C_L	lift coefficient $\left(\frac{\text{twice semispan lift}}{qS} \right)$
C_m	pitching-moment coefficient, referred to 0.25 \bar{c} $\left(\frac{\text{twice semispan pitching moment}}{qS\bar{c}} \right)$
A	aspect ratio $\left(\frac{b^2}{S} \right)$
$\frac{L}{D}$	lift-drag ratio
$\left(\frac{L}{D} \right)_{\max}$	maximum lift-drag ratio
M	Mach number
R	Reynolds number based on wing mean aerodynamic chord

S	total wing area (twice wing area of semispan model), square feet
V	velocity, feet per second
b	twice span of semispan model, feet
c	local chord, feet
\bar{c}	mean aerodynamic chord $\left(\frac{\int_0^{b/2} c^2 dy}{\int_0^{b/2} c dy} \right)$, feet
q	dynamic pressure $\left(\frac{1}{2} \rho V^2 \right)$, pounds per square foot
y	spanwise distance from plane of symmetry, feet
α	angle of attack, degrees
ρ	air density, slugs per cubic foot
$\frac{dC_L}{d\alpha}$	slope of lift curve measured at zero lift, per degree
$\frac{dC_m}{dC_L}$	slope of pitching-moment curve measured at zero lift

APPARATUS AND MODELS

The models were tested on a transonic bump in the Ames 16-foot high-speed wind tunnel. A description of the bump may be found in reference 4. Aerodynamic forces and moments were measured by means of an electrical strain-gage balance mounted inside the bump.

Figure 1 presents photographs of two of the models mounted on the bump, and plan-view drawings of the models are presented as figure 2. The trapezoidal wing was obtained by cutting the tip from the aspect ratio 3 triangular wing.

The following table presents pertinent dimensional data.

	Triangular wings		Trapezoidal wing
	2	3	2
Aspect ratio	2	3	2
Semispan wing area, ft ²	0.250	0.375	0.360
Mean aerodynamic chord, ft	0.667	0.667	0.689
Fence area, ft ²	0.256	0.256	0.256
Wing section, streamwise	NACA 0003-63 NACA 0005-63	NACA 0003-63	NACA 0003-63

A fence—(2.75 in. wide and 14 in. long with semicircular ends) located 3/16 inch from the bump surface was used to reduce the effects of leakage which resulted from clearance between the wing and bump surface required for this type of mounting.

The ratio of fence area to semispan wing areas was as follows:

	Aspect ratio	Fence area
		Semispan wing area
Triangular wings	2	1.02
	3	.68
Trapezoidal wing	2	.71

TESTS AND PROCEDURE

Range of Variables

The aerodynamic characteristics of the wings were investigated over a Mach number range from 0.60 to 1.10. The variation of test Reynolds number with Mach number is shown in figure 3. The angle-of-attack range extended from -6° to an angle limited by the capacity of the strain gages.

Reduction of Data

Typical Mach number contours of the flow over the bump without a model in place are shown in figure 4. The outline of the aspect ratio 2 wings are superposed to indicate the Mach number variation over the model. No account has been taken of the Mach number variation over the model. The test Mach number was taken to be the Mach number of the contour passing through the 25-percent point of the mean aerodynamic chord.

The drag data were corrected to account for an interaction between the lift and drag components of the balance. A tare correction to the drag to account for the fence drag was evaluated by testing a fence alone. The measured fence tare drag was independent of angle of attack. Tare drag coefficients based on the wing area are listed below:

Mach number	0.60 through 0.98	1.02	1.06 through 1.10
Aspect ratio 2, triangular wings	0.0050	0.0059	0.0066
Aspect ratio 3, triangular wing	.0035	.0038	.0044
Aspect ratio 2, trapezoidal wing	.0036	.0040	.0046

An angle-of-attack correction of -0.4° was included to account for the cross flow over the bump. Interference effects of the fence and effects of leakage around the fence are not known and no corrections for these effects have been made. A boundary layer, which is approximately $3/4$ inch thick at the location of the model, exists over the surface of the transonic bump. No account has been taken of its effect on the aerodynamic characteristics.

RESULTS AND DISCUSSION

Lift, drag, pitching moment, and lift-drag ratio for each of the four wings investigated are shown in figures 5 through 8. Data obtained from investigations in the Ames 12-foot and 6- by 6-foot wind tunnels of similar wings in combination with a body have been included. The 6- by 6-foot tunnel data included herein were obtained over a Mach number

range from 0.60 to 0.90 and 1.3 to 1.7 at a Reynolds number of 3.0 million for the aspect ratio 2 wings, and over a Mach number range from 0.60 to 0.92 and 1.2 to 1.7 at a Reynolds number of 4.8 million for the aspect ratio 3 wing. Data from the 12-foot tunnel that are included herein were obtained over a Mach number range from 0.24 to 0.95 at a Reynolds number of 3.0 million. Summary data as a function of Mach number for the four wings are shown in figure 9. The slope parameters in this figure have been measured at zero lift.

The fact that the data obtained in the 6- by 6-foot and 12-foot wind tunnels are for wing-body combinations precludes a direct comparison with the results obtained for the wing alone. The theory of reference 5, however, predicts that it would be reasonable to expect a lift decrement in the case of the wing-body combination. The results presented in part (a) of figures 5, 6, 7, and 9 show the opposite effect. In the present bump investigation it is concluded that the effects of leakage and bump boundary layer could be responsible for the reduction in lift. The results presented in figure 9(a) show that there is a maximum of 4-percent difference in lift-curve slope between the 3- and 5-percent-thick triangular wings of aspect ratio 2. An expected increase in lift-curve slope accompanied an increase in aspect ratio. It is interesting to note that the aspect ratio 3 triangular wing after modification to the trapezoidal wing of aspect ratio 2 retained greater lift-curve slope than the aspect ratio 2 triangular wings.

Examination of figure 9(b) shows the variation of drag coefficient with Mach number to be somewhat irregular but certain trends are evident. At the lower Mach numbers of 0.60 and 0.70 under conditions of lift, the drag of the 3-percent-thick, aspect ratio 2 wing is higher than the 5-percent-thick, aspect ratio 2 wing and, characteristically, the drag of the thicker wing rises to a higher value at Mach numbers above approximately 1.0. The aspect ratio 3 wing under conditions of lift had considerably less drag than either of the aspect ratio 2 triangular wings. Modification of the aspect ratio 3 wing to an aspect ratio 2 trapezoidal wing, in general, increased the drag except below a Mach number of 0.75 and below a lift coefficient of 0.2. Under these conditions the drag of the trapezoidal wing was less than that of the aspect ratio 3 wing, and above a lift coefficient of 0.2 it was less than that of the aspect ratio 2 triangular wings.

In general, the models tested in the 16-foot tunnel were more stable than those tested in either of the other tunnels, as may be seen in part (c) of figures 5, 6, 7, and 9. This is to be expected because of the generally destabilizing influence of the body. At a Mach number of 0.90 at high lift, however, the data indicate that the triangular wings having the NACA 0003-63 section were less stable alone than when tested with a body. The pitching-moment data from the 16-foot tunnel for the 3-percent-thick, aspect ratio 2 triangular wing and the trapezoidal

wing do not show the abrupt, unstable break that occurs for the 3-percent-thick, aspect ratio 3 wing and the 5-percent-thick, aspect ratio 2 wing between lift coefficients of 0.4 and 0.7. Data shown in figure 5(c) for the 5-percent-thick, aspect ratio 2 wing indicate that the other investigations have shown an unstable break in the pitching-moment curve, but not with the same degree of severity. Summary data in figure 9(c) show that the variation of the stability parameter with Mach number was essentially the same for all the wings. Here again thickness had very little effect on the parameter but the aspect ratio 2 wings were more stable than the aspect ratio 3 wing with the exception of the trapezoidal wing. As would be expected, the trapezoidal wing was less stable than any of the other wings because it was produced by removing a portion that made a large contribution to the negative pitching moment of the aspect ratio 3 wing.

The data of figure 9(d) show the variation of maximum lift-drag ratio with Mach number. Supersonically, the thinner, aspect ratio 2 wing was of course more efficient. Above a Mach number of 0.75 the aspect ratio 3 wing was superior to all the others reported herein. The values of maximum lift-drag ratio for the trapezoidal wing were comparable to those for the 3-percent thick, aspect ratio 2 triangular wing above a Mach number of 0.80. At lower Mach numbers, below 0.75, the trapezoidal wing was superior even to the aspect ratio 3 wing.

The trapezoidal wing reported herein was investigated in order to ascertain whether or not the theory of reference 6 was applicable at an aspect ratio of 3. On a coefficient basis examination shows that in order for the trapezoidal wing to conform to the hypothesis that the part of the surface having parallel sides would develop no lift, the lift-curve slope should be 33 percent lower for the trapezoidal wing than that for the aspect ratio 3 wing. This, however, was not the case. The lift-curve slope was reduced, but only by about 15 percent.

A comparison of the aerodynamic characteristics of the trapezoidal wing of aspect ratio 2 and those of the aspect ratio 2 triangular wing of the same thickness-to-chord ratio reveals that minimum drag values were essentially the same; however, the trapezoidal wing had the higher lift-curve slope, lower drag due to lift, a higher maximum lift-drag ratio below a Mach number of 0.80, but a lower maximum lift-drag ratio above a Mach number of 0.80, and a greater center-of-pressure travel.

In general, the foregoing points out that the aspect ratio 2 trapezoidal wing had aerodynamic characteristics superior to those of an aspect ratio 2 triangular wing.

Carrying the comparison further, it can be seen that the aspect ratio 2 trapezoidal wing when compared with the aspect ratio 3 triangular wing of the same thickness-to-chord ratio had slightly higher minimum drag

values above a Mach number of 0.80, lower lift-curve slope, lower values of maximum lift-drag ratio above a Mach number of 0.75, higher drag due to lift, and a greater center-of-pressure travel. Thus clipping the wing tips did not improve the aerodynamic characteristics except below a Mach number of 0.75 at low lift coefficients.

The limited scope of the present investigation cannot lead to any generalized comments regarding the merit of clipping the tips of triangular wings. It is felt, however, that the results of this investigation indicate that beneficial effects may be obtained by removing the tips of triangular wings.

CONCLUDING REMARKS

Within the Mach number range investigated the aspect ratio 3 wing was, in general, superior to the others reported herein. Comparison of the characteristics of the aspect ratio 2 triangular wings showed little difference between the 3-percent and the 5-percent-thick wings below a Mach number of 1.0, while above a Mach number of 1.0 the 3-percent-thick wing had superior aerodynamic characteristics.

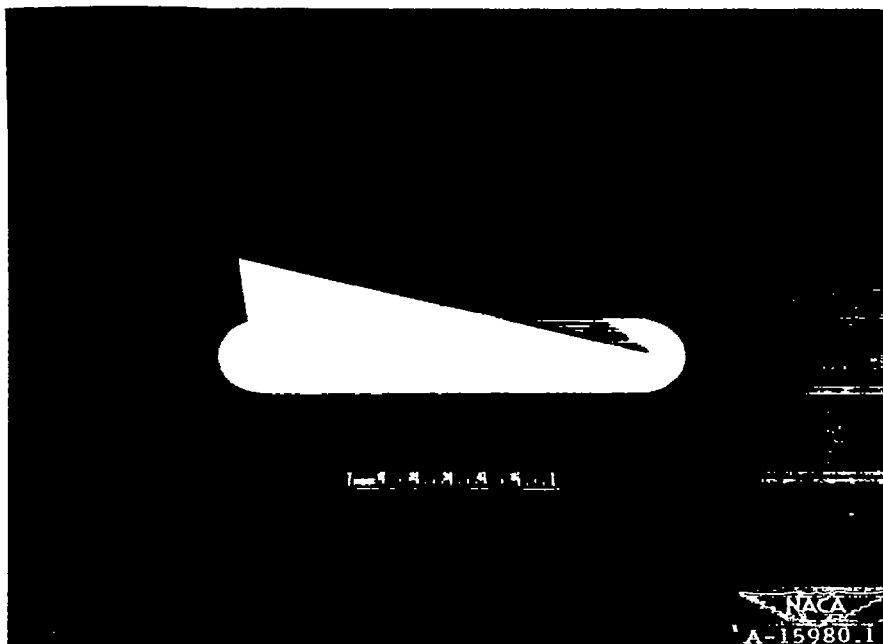
Modification of the aspect ratio 3 wing to an aspect ratio 2 trapezoidal wing had a deleterious effect on the aerodynamic characteristics at Mach numbers above 0.75 but a beneficial effect at lift coefficients below 0.2 and Mach numbers below 0.75. The aerodynamic characteristics of the trapezoidal wing, however, were the same as or superior to those of the aspect ratio 2 triangular wings.

Ames Aeronautical Laboratory
National Advisory Committee for Aeronautics
Moffett Field, Calif.

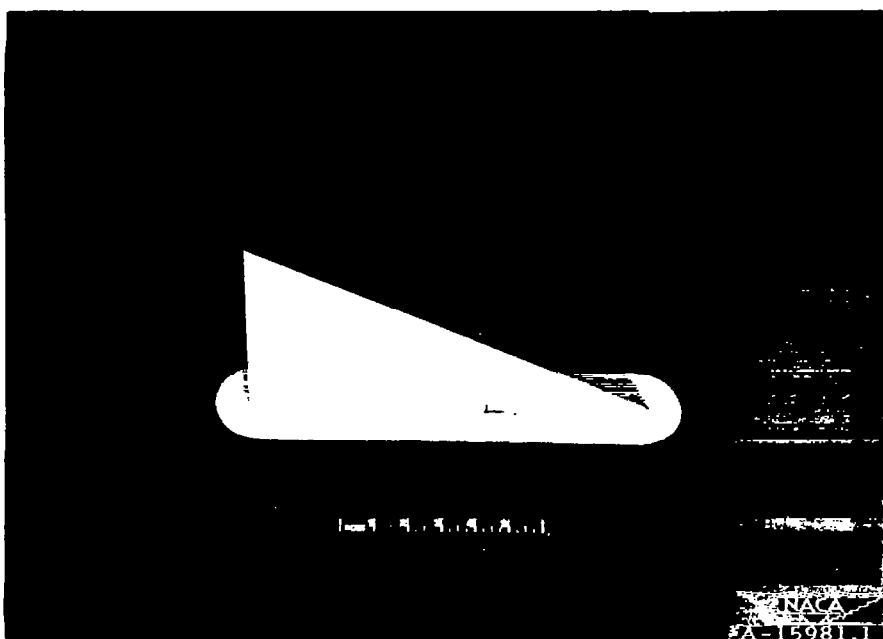
REFERENCES

1. Smith, Donald W., and Heitmeyer, John C.: Lift, Drag, and Pitching Moment of Low-Aspect-Ratio Wings at Subsonic and Supersonic Speeds - Plane Triangular Wing of Aspect Ratio 2 With NACA 0005-63 Section. NACA RM A50K21, 1951.
2. Heitmeyer, John C., and Smith, Willard G.: Lift, Drag, and Pitching Moment of Low-Aspect-Ratio Wings at Subsonic and Supersonic Speeds - Plane Triangular Wing of Aspect Ratio 2 With NACA 0003-63 Section. NACA RM A50K24a, 1951.

3. Heitmeyer, John C.: Lift, Drag, and Pitching Moment of Low-Aspect-Ratio Wings at Subsonic and Supersonic Speeds, - Plane Triangular Wing of Aspect Ratio 3 With NACA 0003-63 Section. NACA RM A51H02, 1951.
4. Axelson, John A., and Taylor, Robert A.: Preliminary Investigation of the Transonic Characteristics of an NACA Submerged Inlet. NACA RM A50C13, 1950.
5. Spreiter, John R.: The Aerodynamic Forces on Slender Plane- and Cruciform-Wing and Body Combinations. NACA Rep. 962, 1950. (Formerly NACA TN's 1662 and 1897)
6. Jones, R.T.: Properties of Low-Aspect-Ratio Pointed Wings at Speeds Below and Above the Speed of Sound. NACA Rep. 835, 1946. (Formerly NACA TN 1032 and ACR L5F13)



(a) Aspect ratio 2.



(b) Aspect ratio 3.

Figure 1.— Photographs of the models with the NACA 0003-63 section mounted on the Ames 16-foot high-speed wind-tunnel bump.

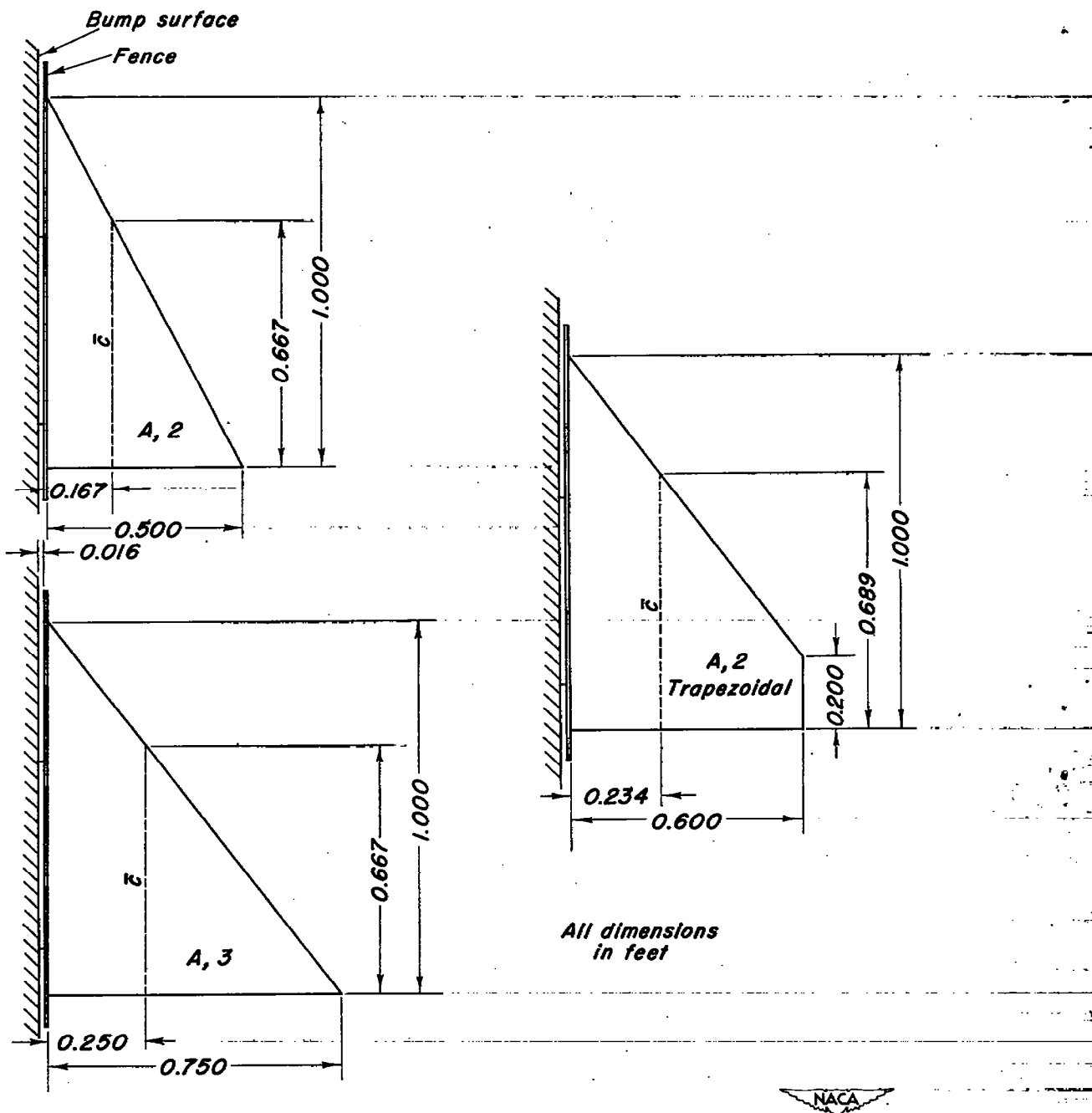


Figure 2.—A plan-view drawing of the wing models.

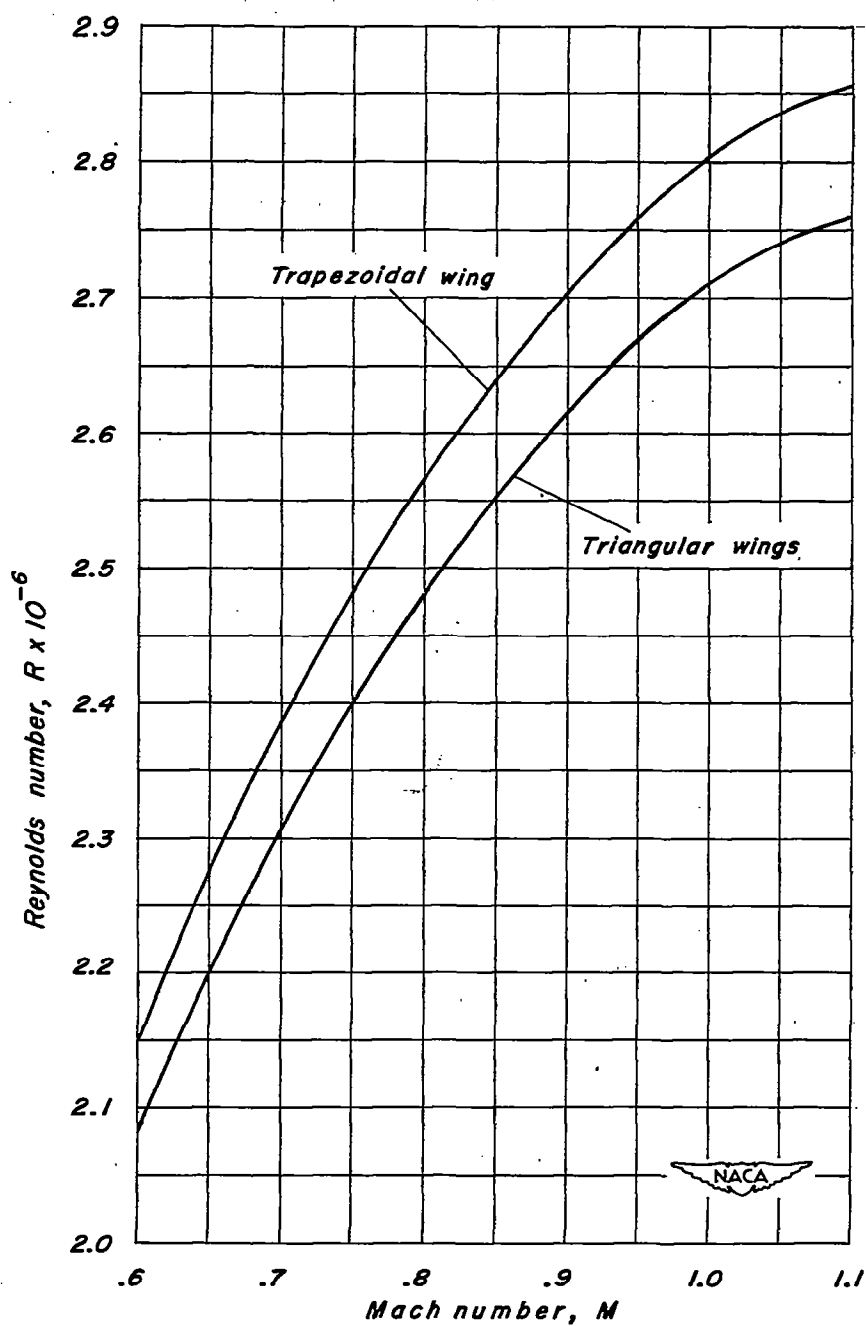


Figure 3.—Variation of Reynolds number with Mach number.

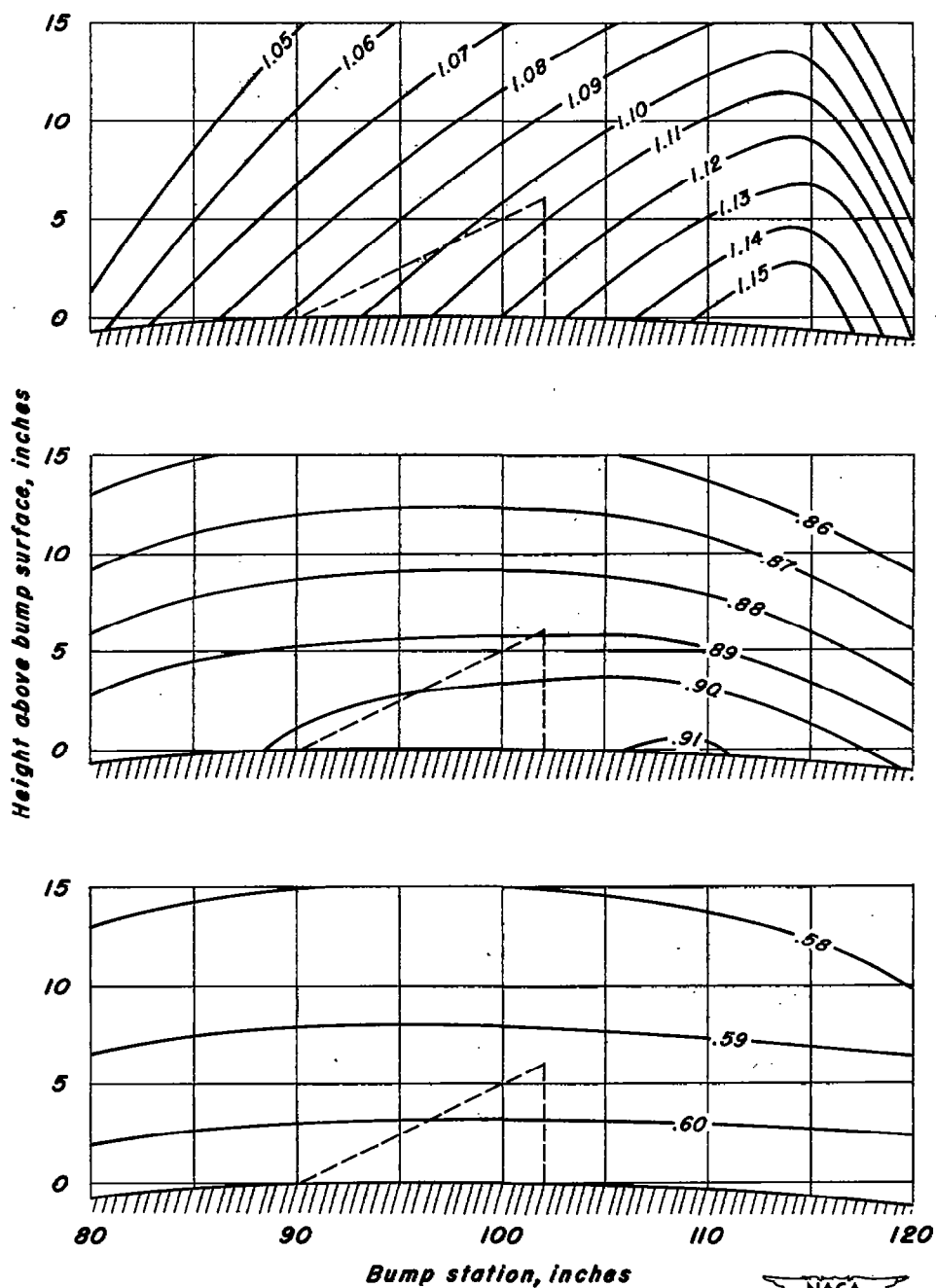
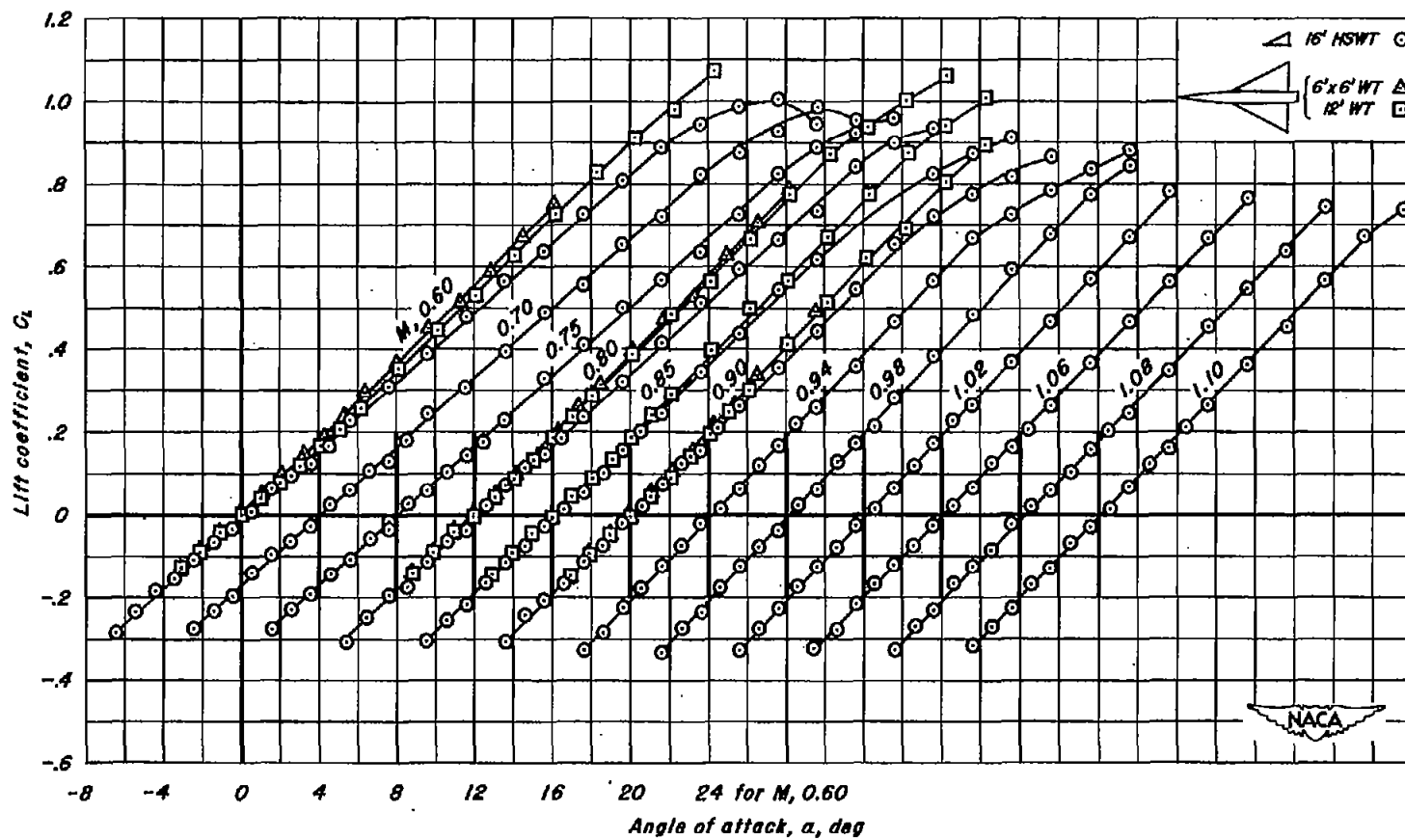


Figure 4.—Typical Mach number contours over the transonic bump in the Ames 16-foot high-speed wind tunnel.



(a) C_L vs α

Figure 5.-The aerodynamic characteristics of the wing of aspect ratio 2 having the NACA 0005-63 section.

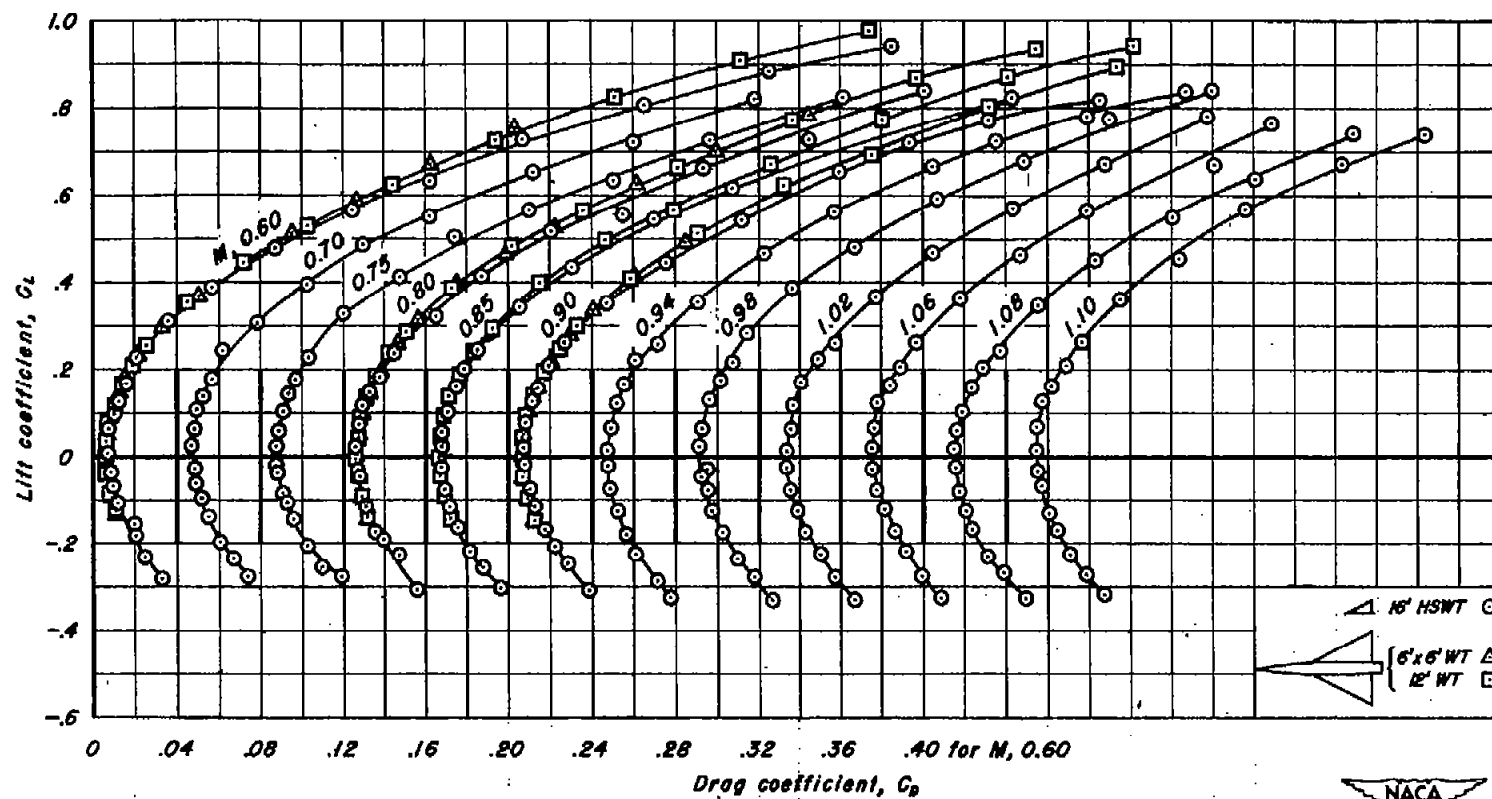
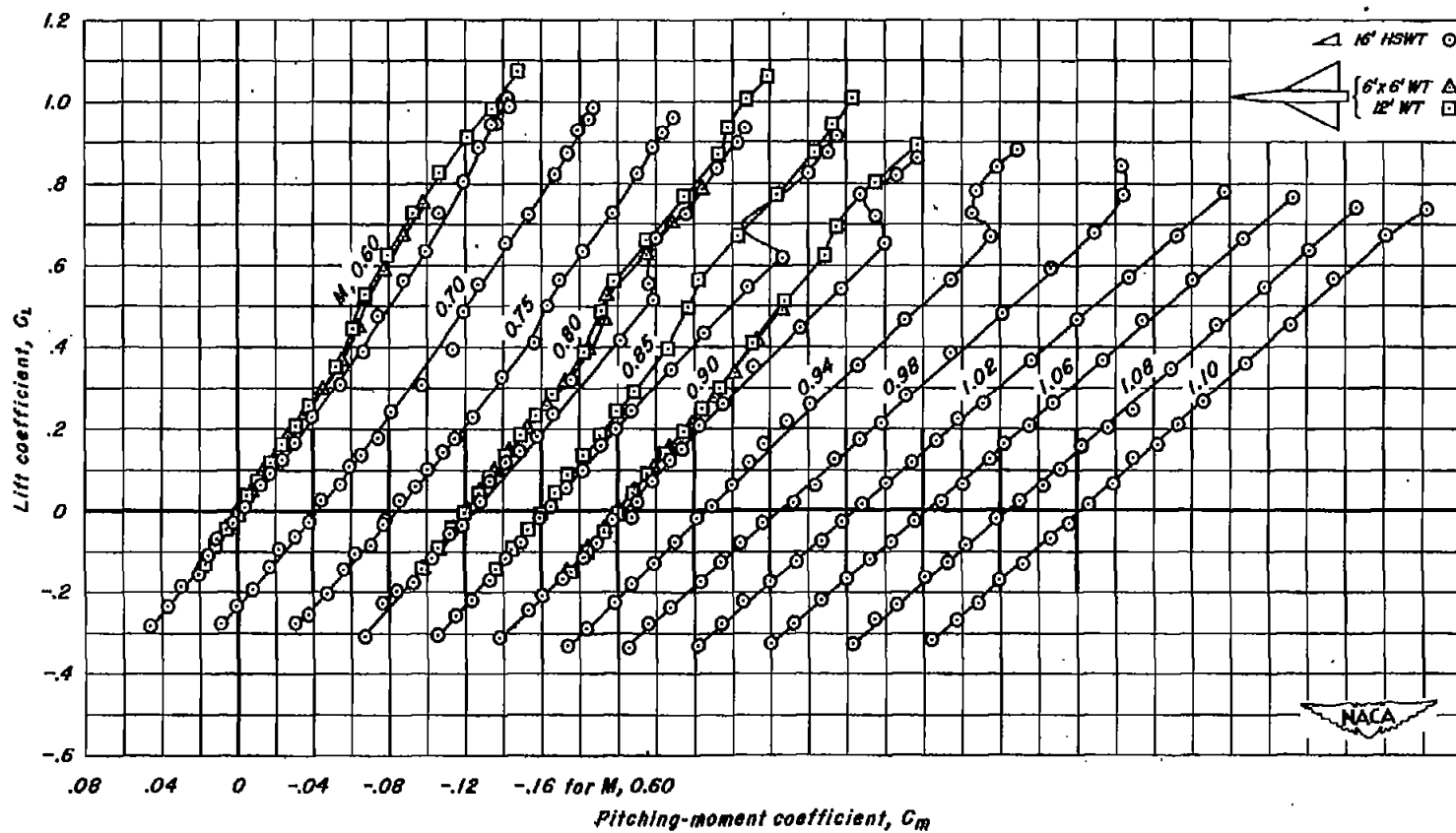
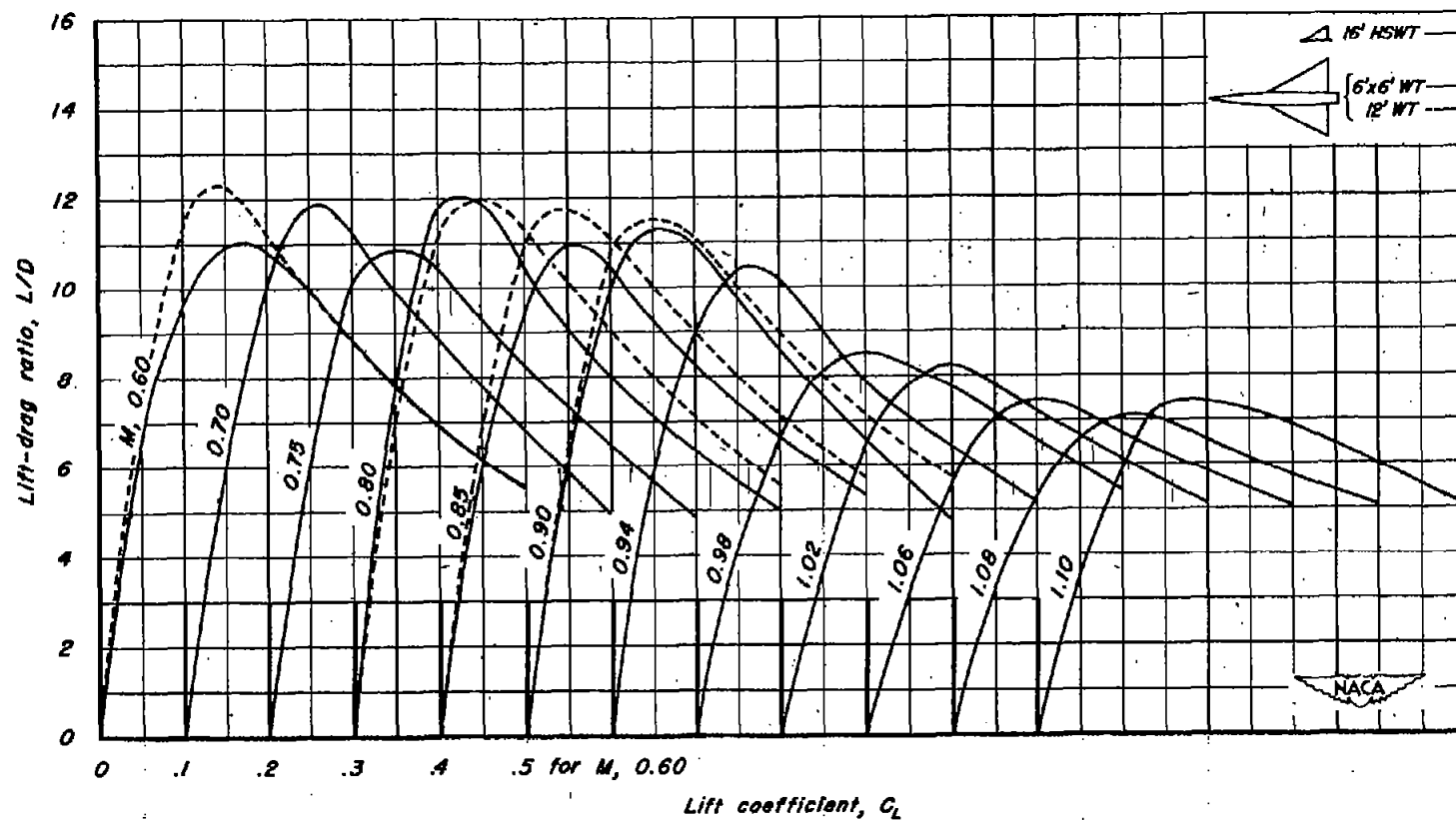
(b) C_L vs C_D

Figure 5.-Continued.



(c) C_L vs C_m

Figure 5.- Continued.



(d) L/D vs C_L

Figure 5.- Concluded.

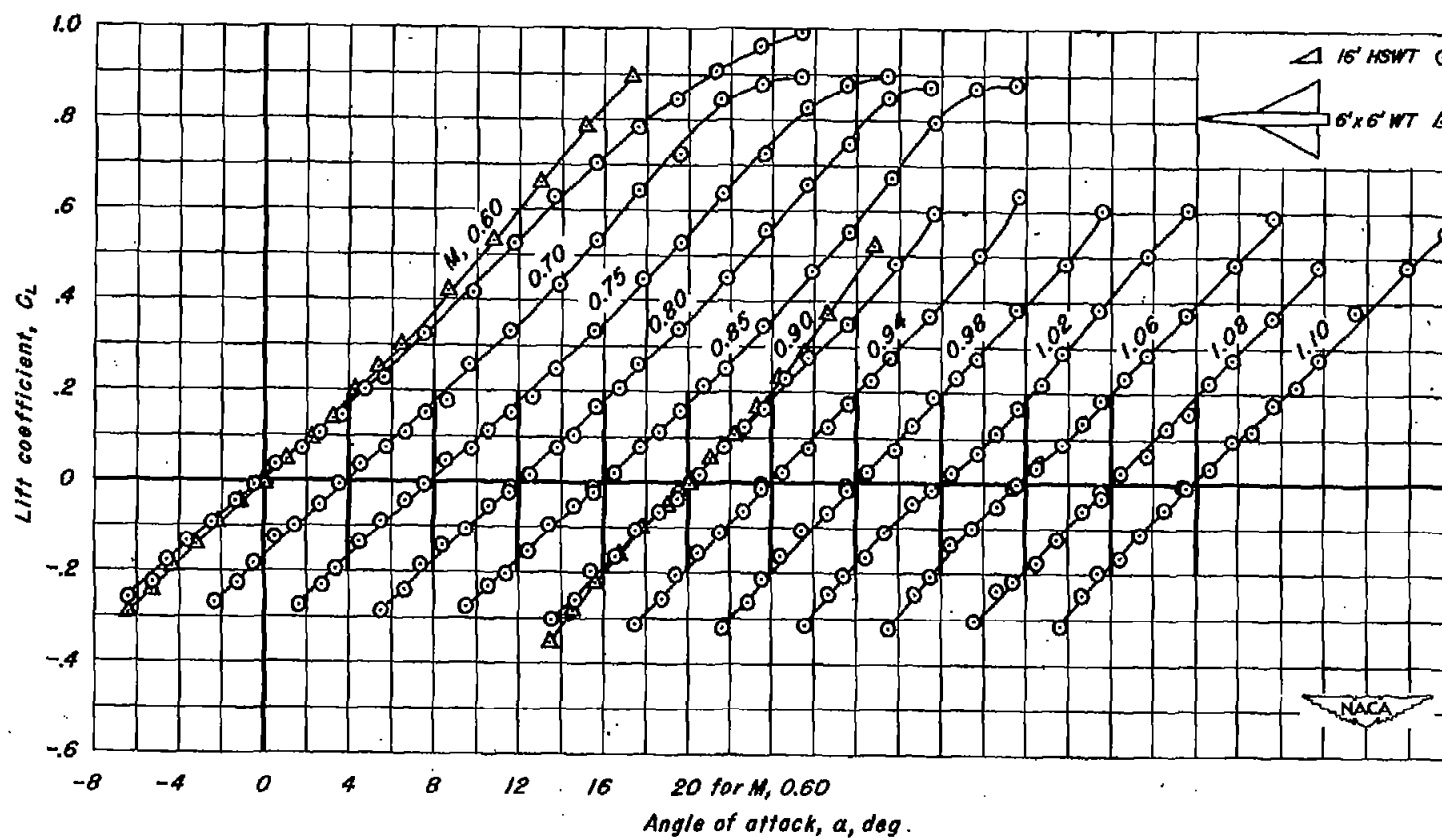
(a) C_L vs α

Figure 6.—The aerodynamic characteristics of the wing of aspect ratio 2 having the NACA 0003-63 section.

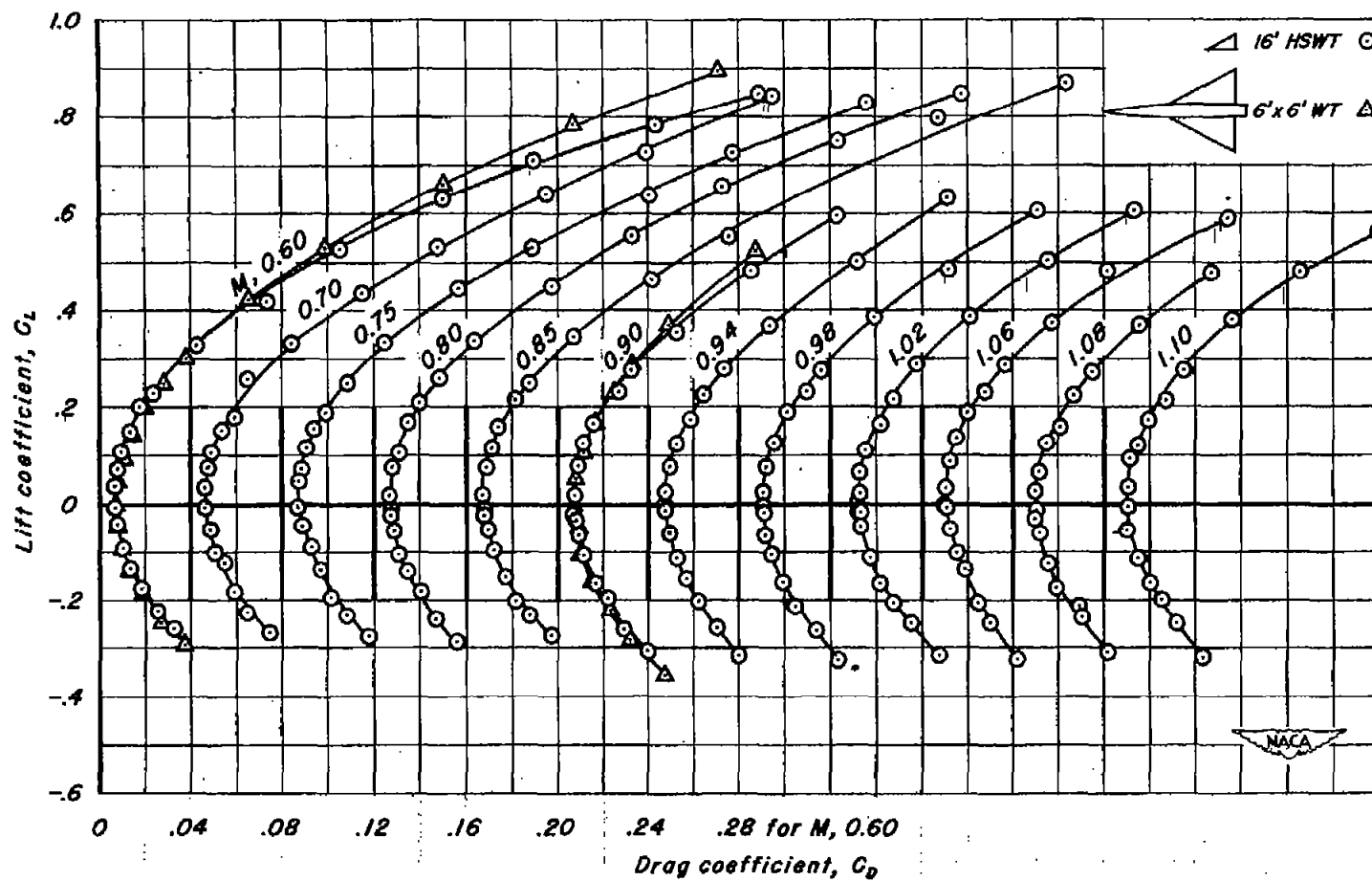
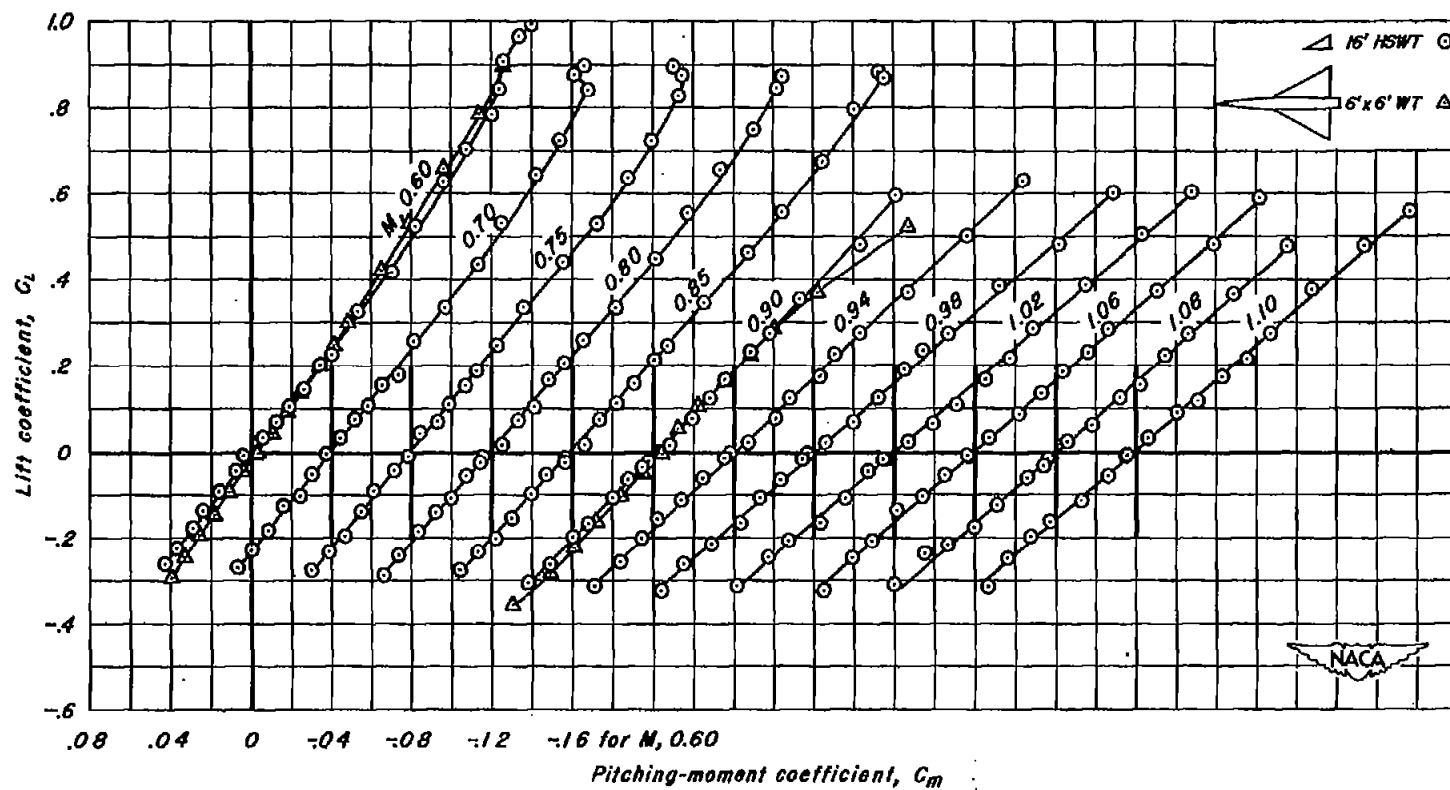
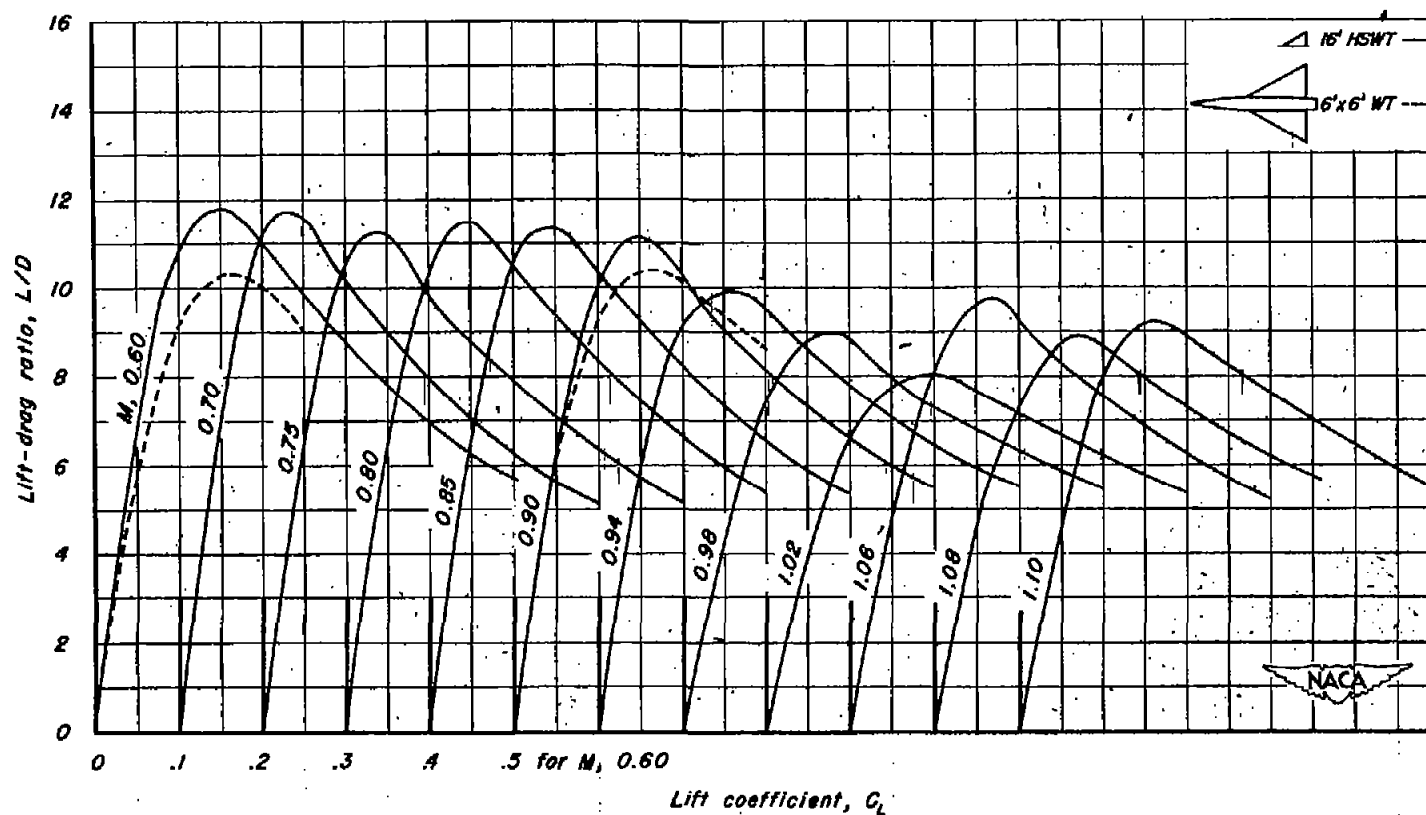
(b) C_L vs C_D

Figure 6.- Continued.



(c) C_L vs C_m

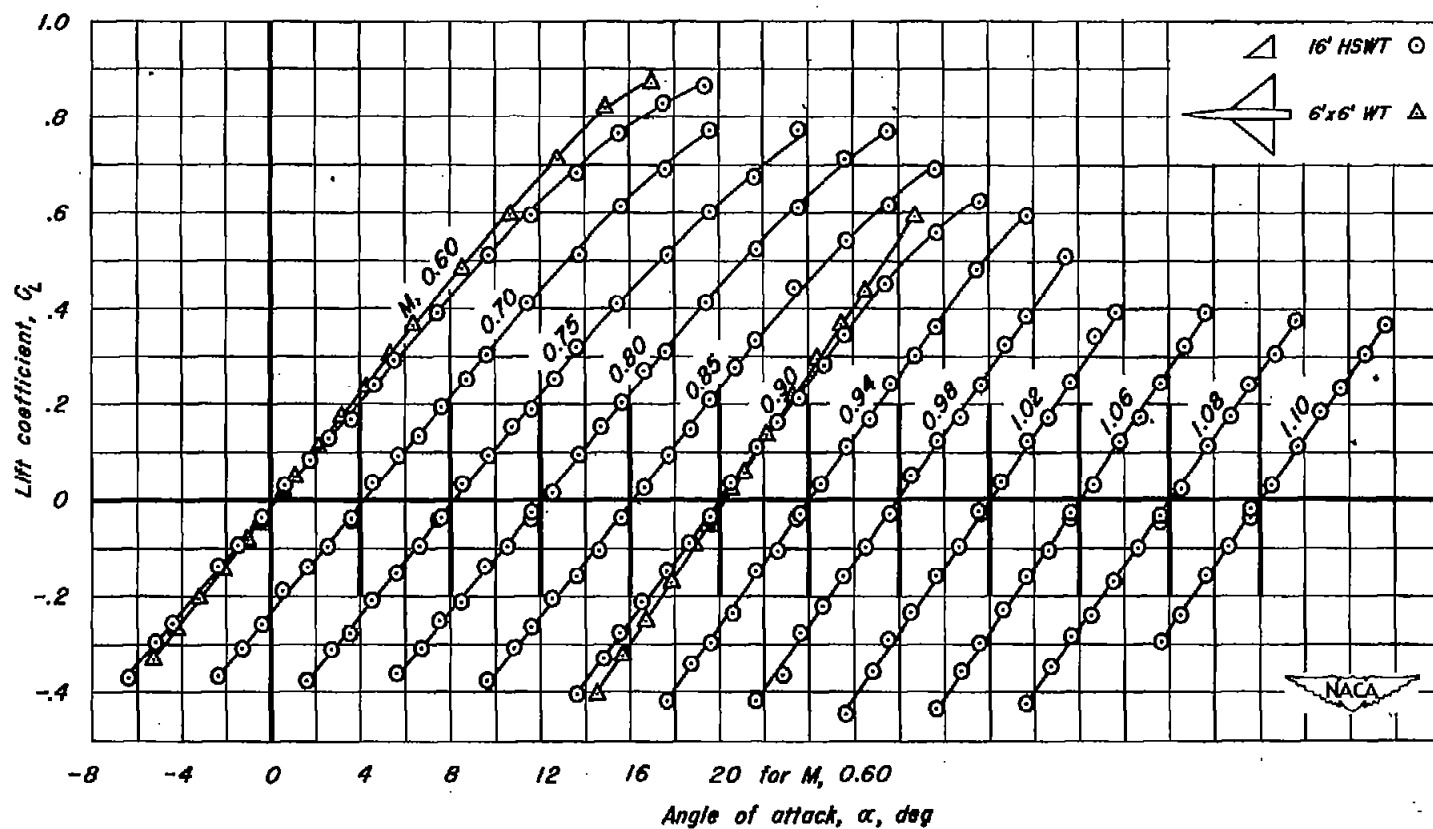
Figure 6.-Continued.



Lift coefficient, C_L

(d) L/D vs C_L

Figure 6.-Concluded.



(a) C_L vs α

Figure 7.—The aerodynamic characteristics of the wing of aspect ratio 3 having the NACA 0003-63 section.

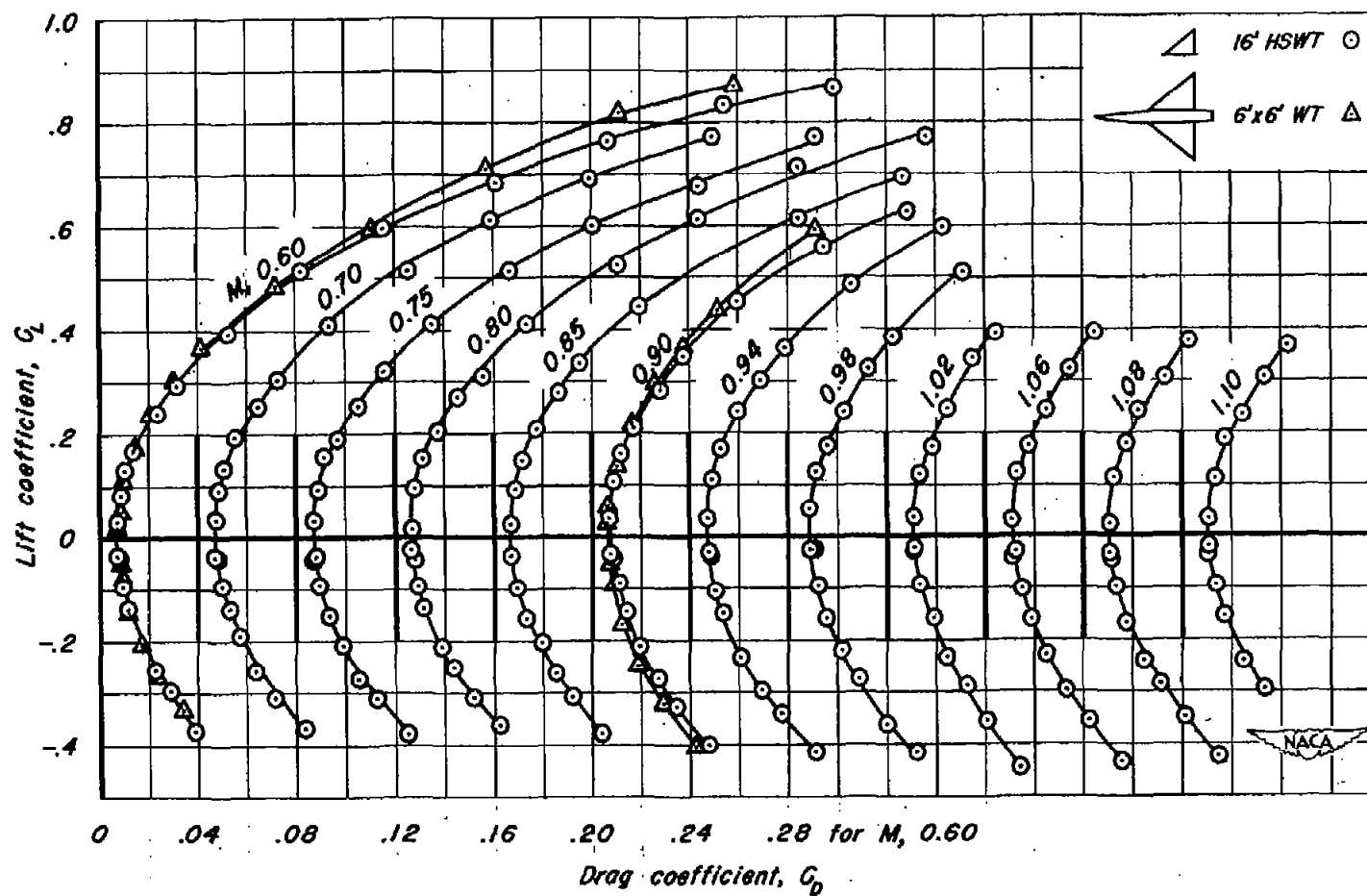
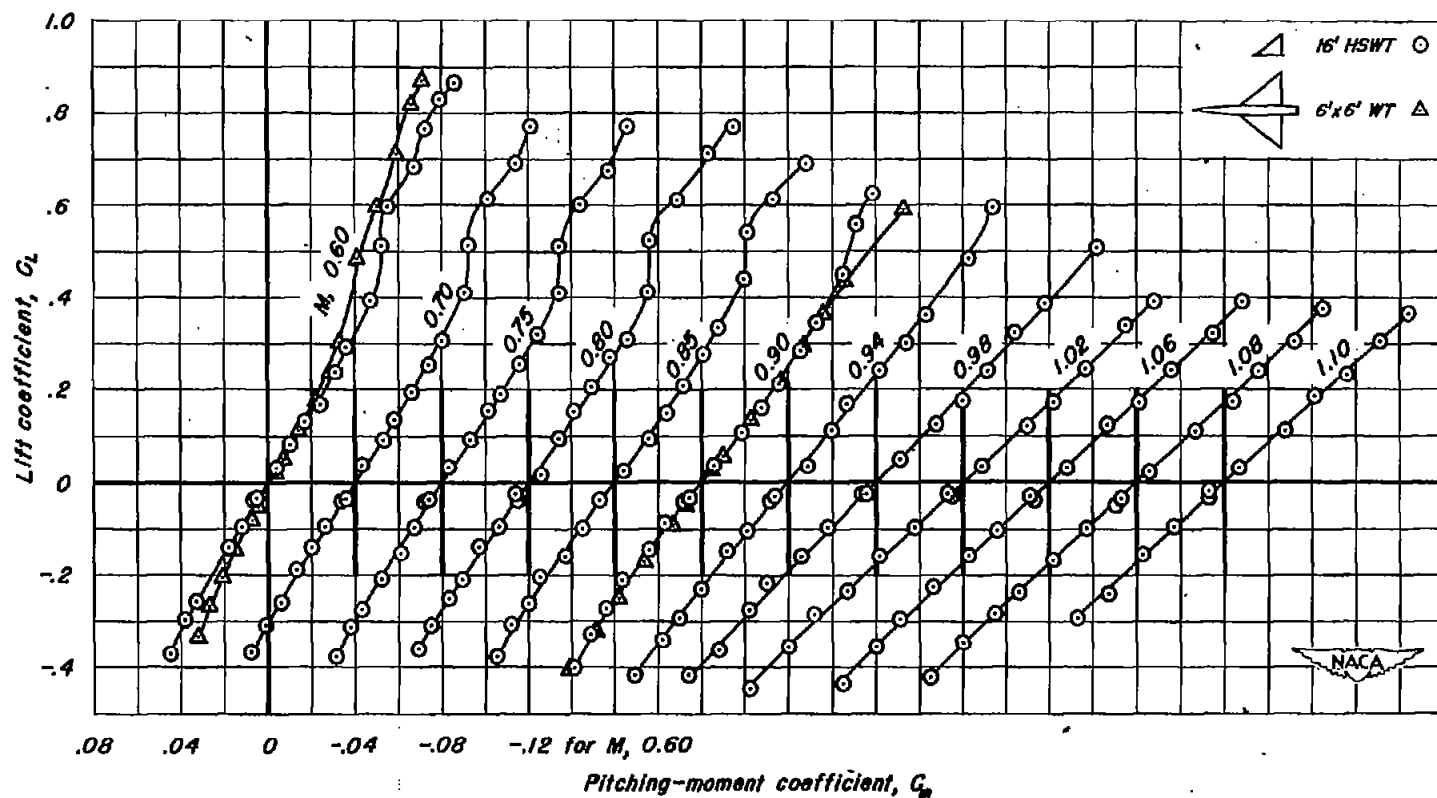
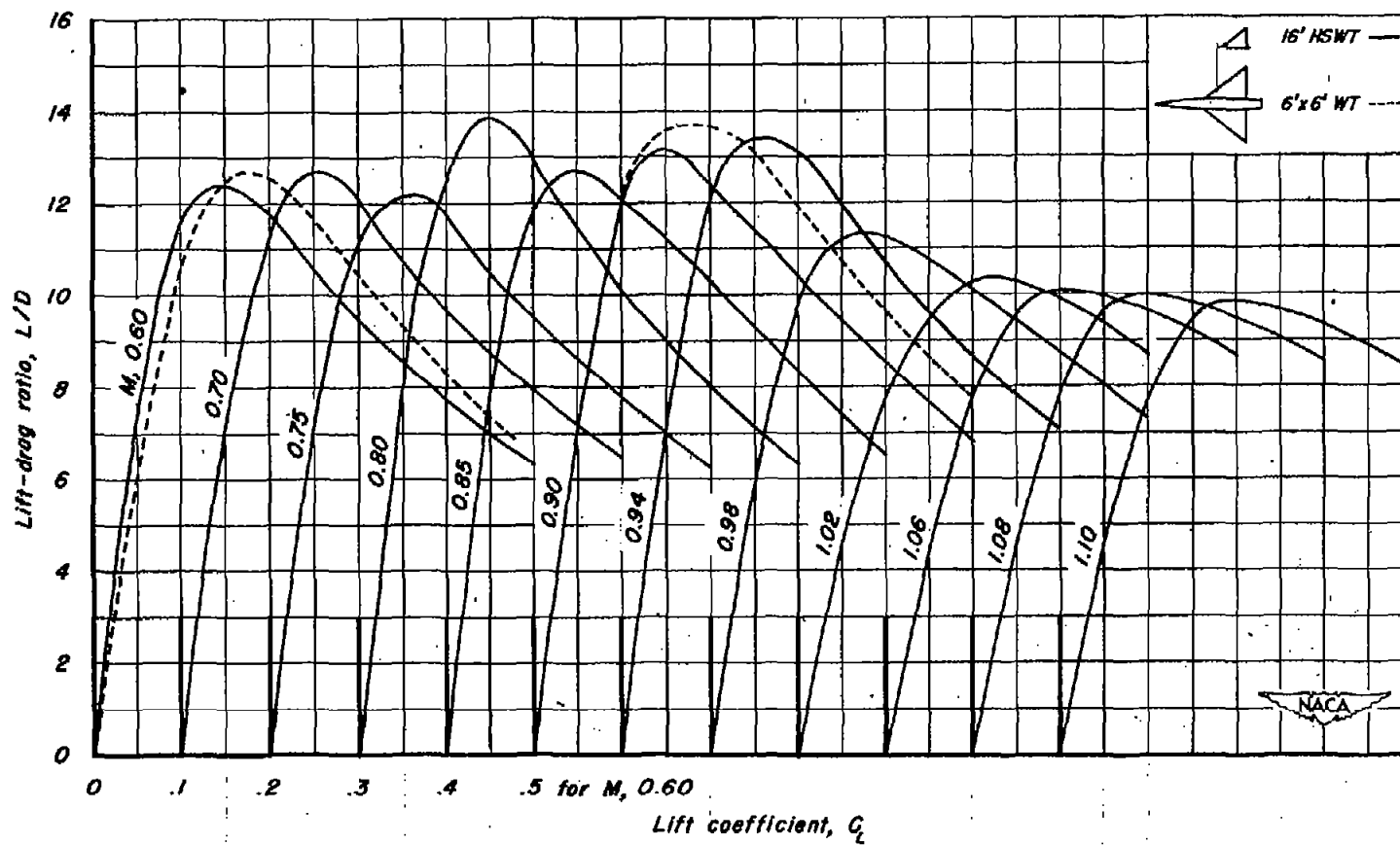
(b) C_L vs C_D

Figure 7.- Continued.



(c) C_L vs C_m

Figure 7.- Continued.



(d) L/D vs C_L

Figure 7.- Concluded.

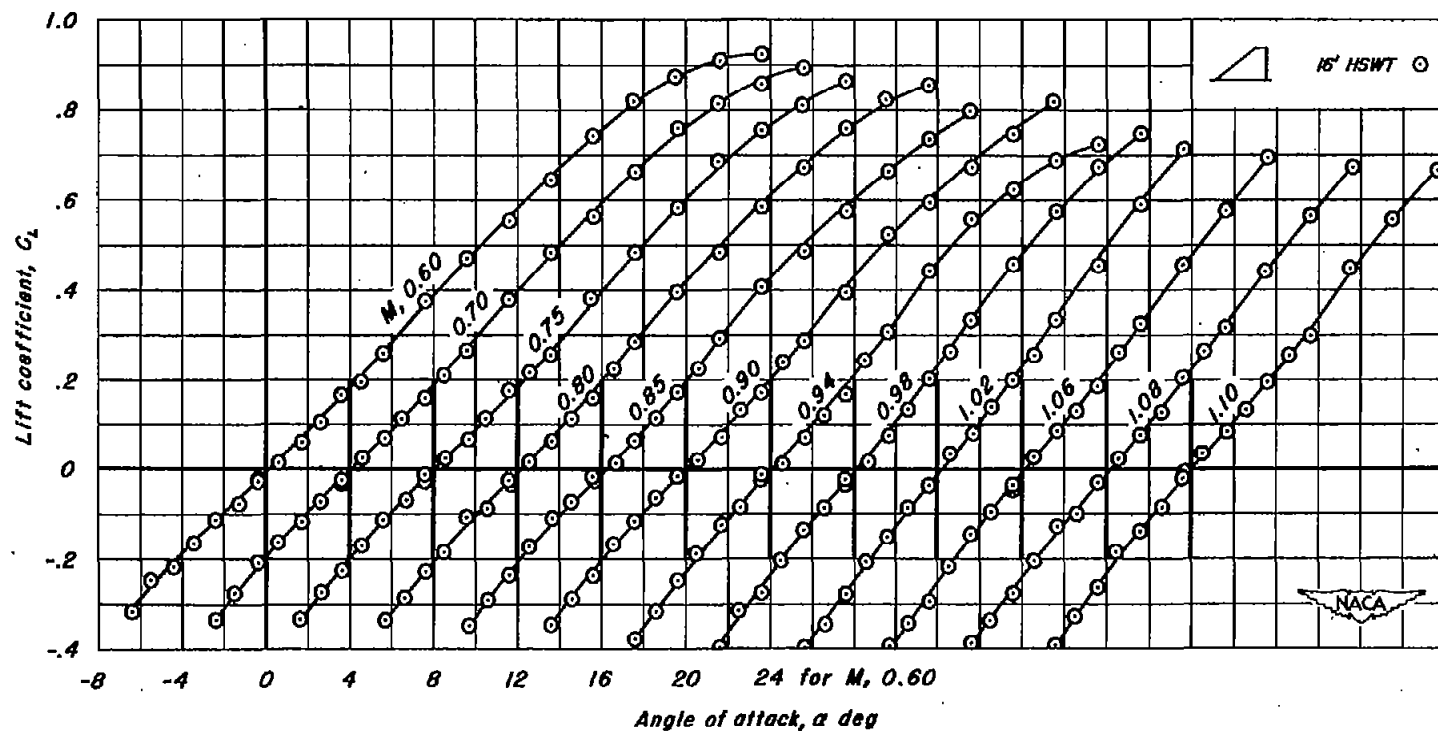
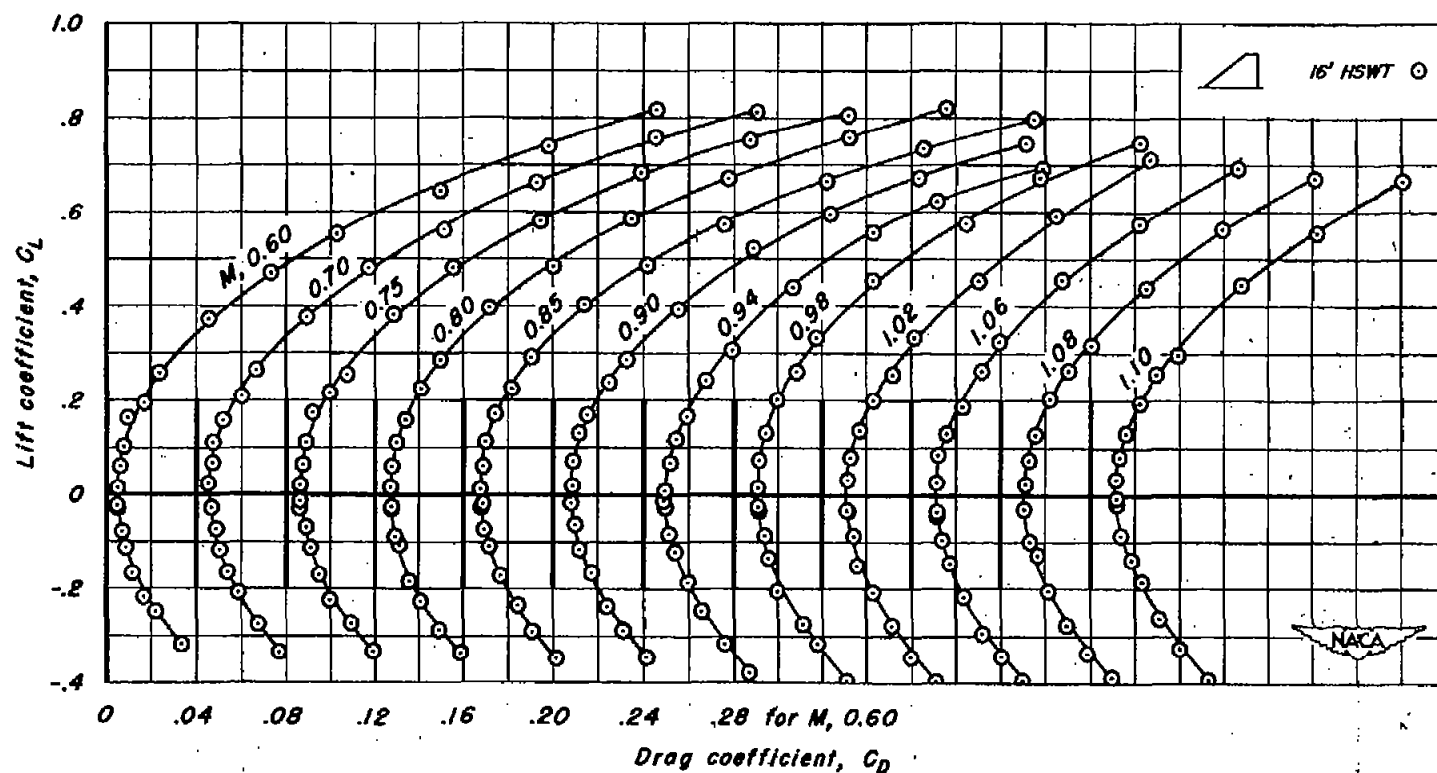
(a) C_L vs α

Figure 8.—The aerodynamic characteristics of the trapezoidal wing.



(b) C_L vs C_D

Figure 8--Continued.

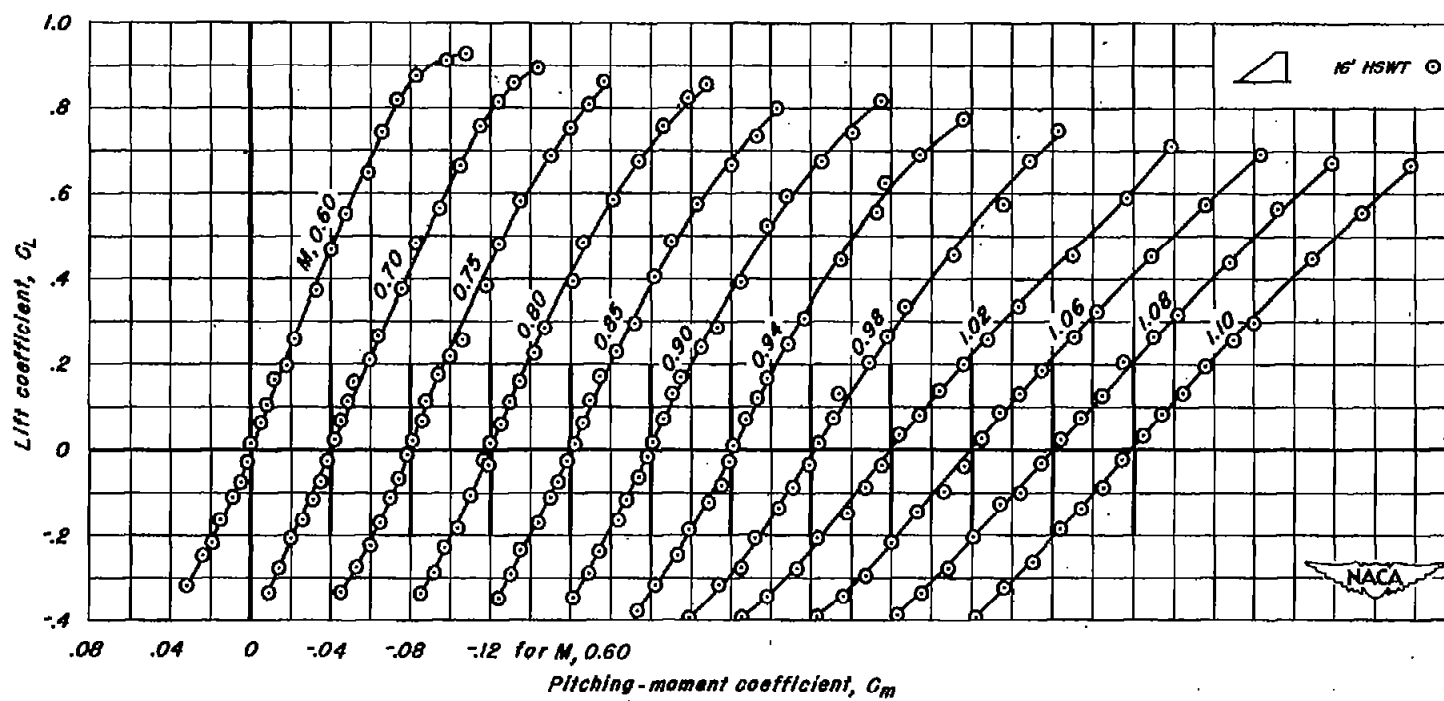
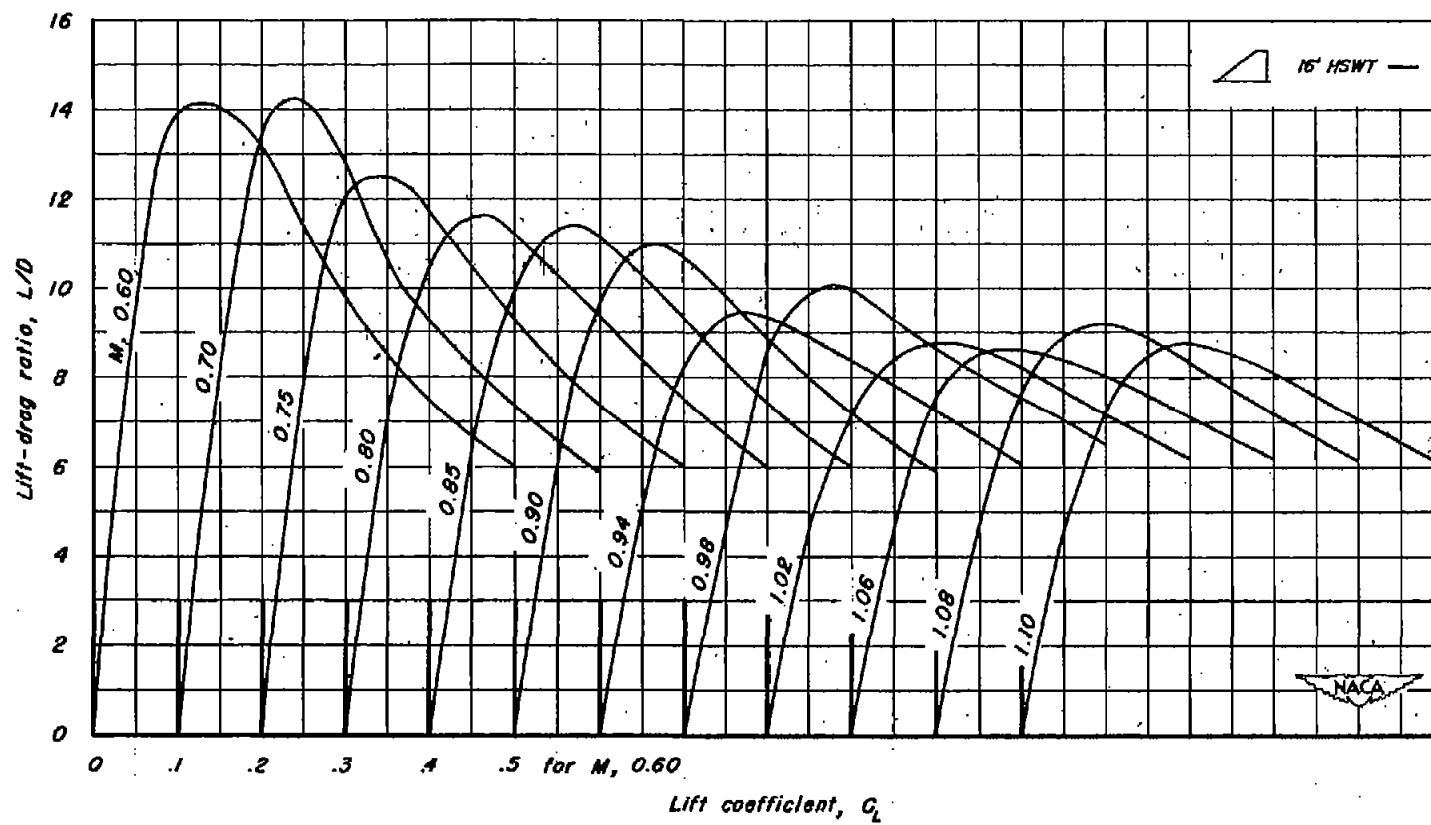
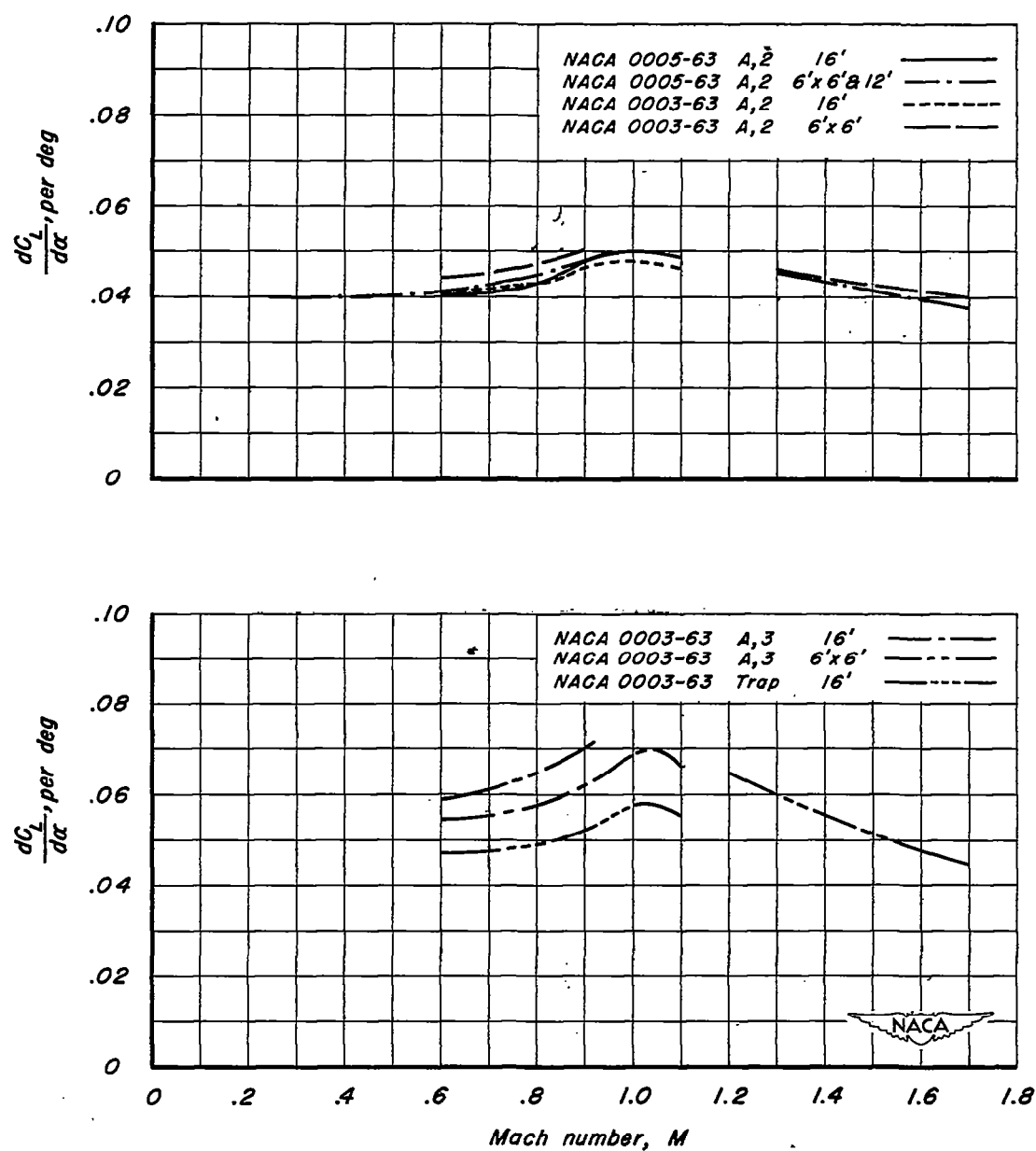
(c) C_L vs C_m

Figure 8--Continued.



(d) L/D vs C_L

Figure B.- Concluded.



(a) $\frac{dC_L}{d\alpha}$ vs M

Figure 9.—Summary of aerodynamic characteristics as a function of Mach number.

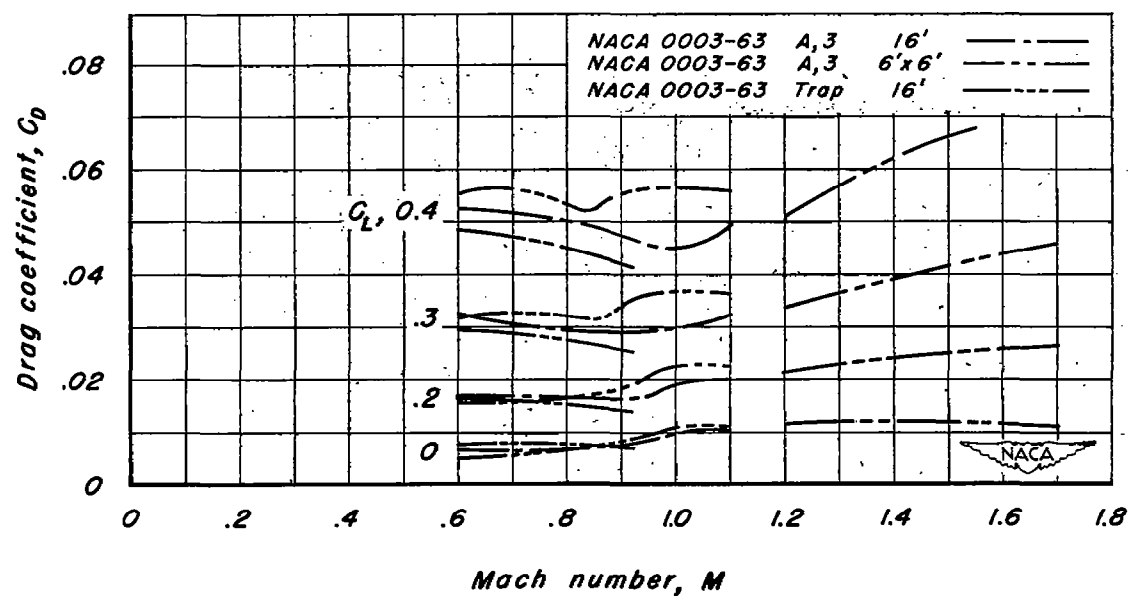
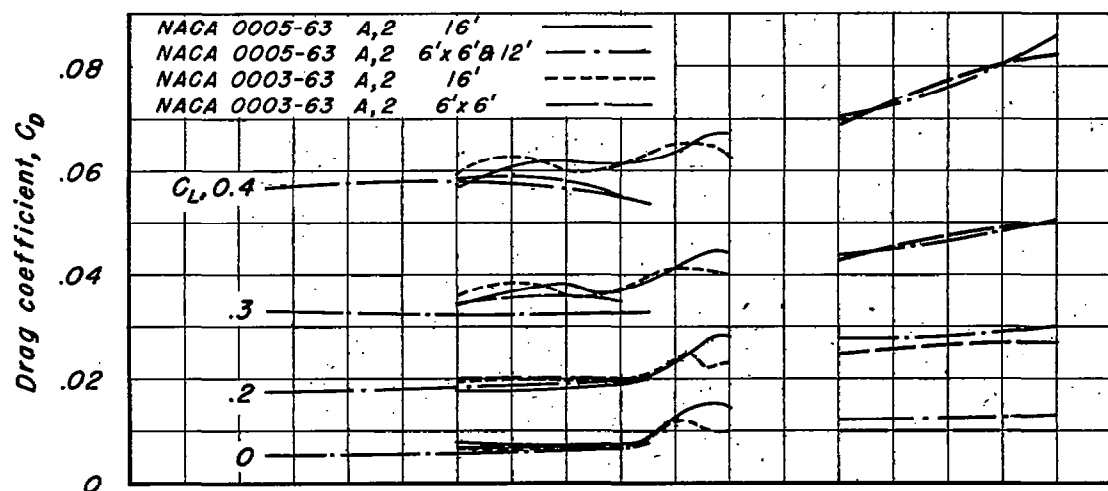
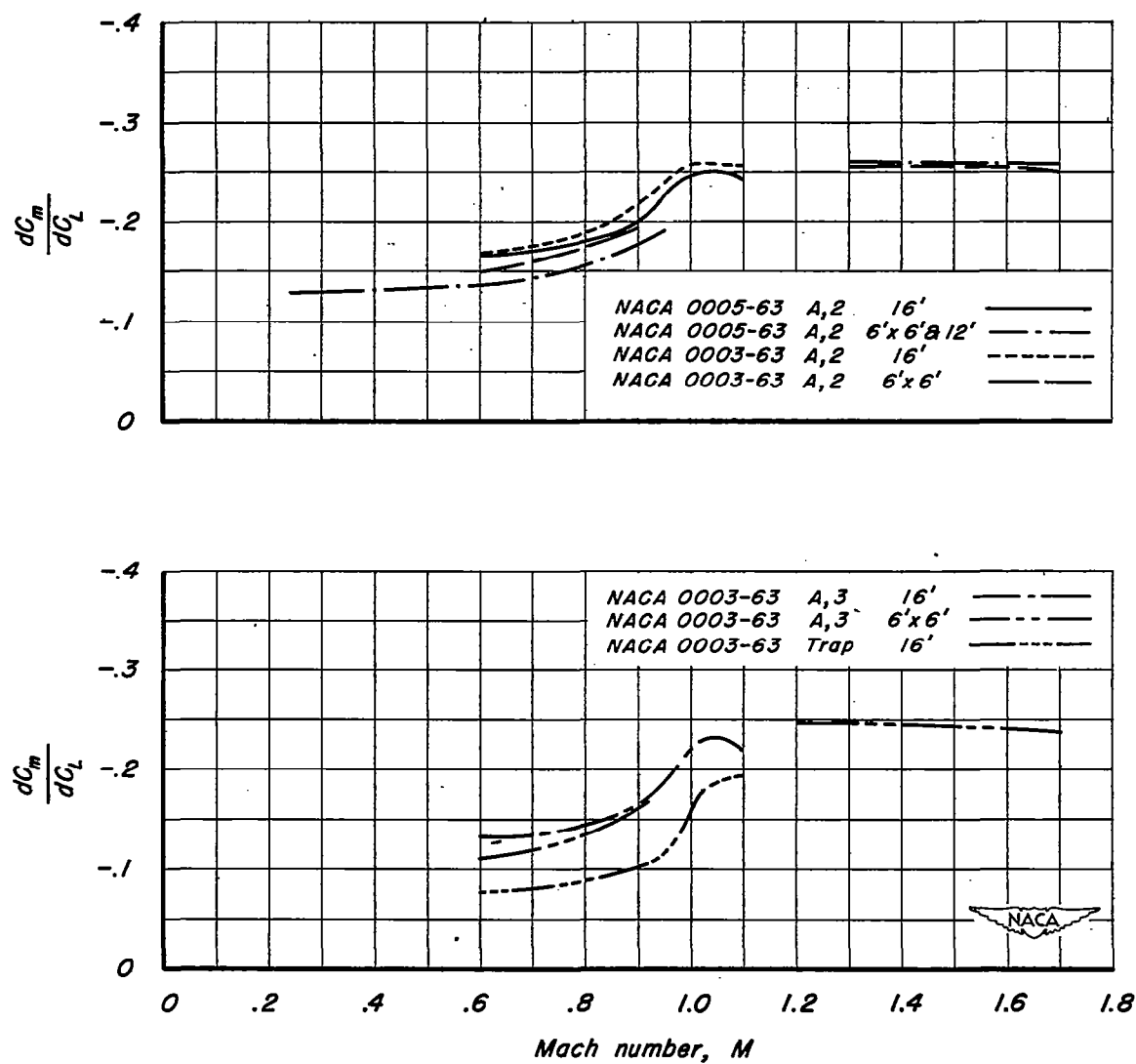
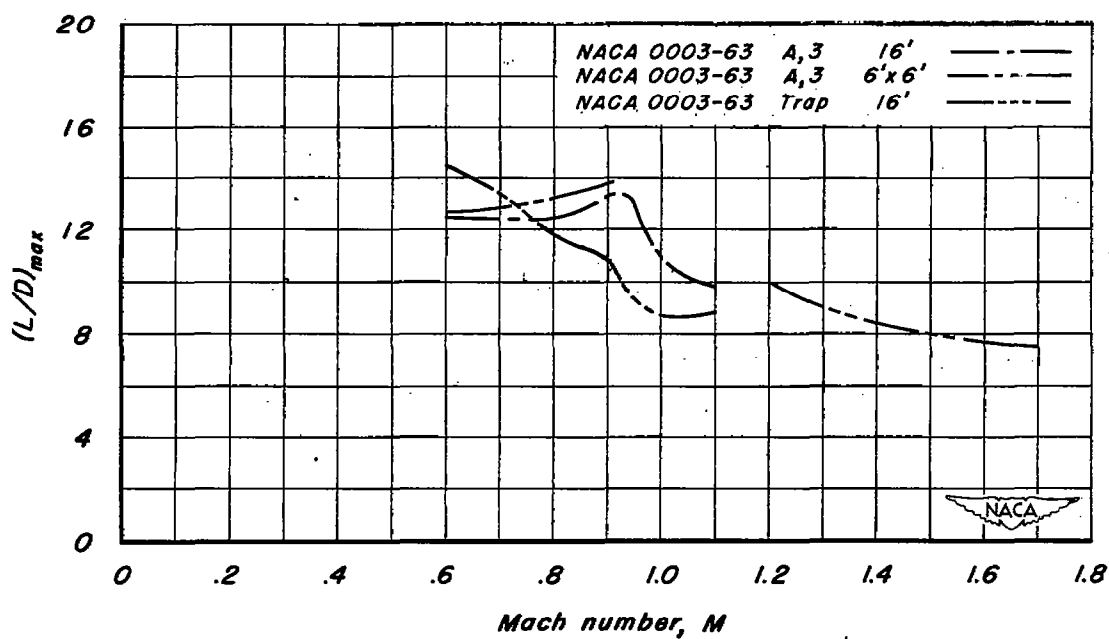
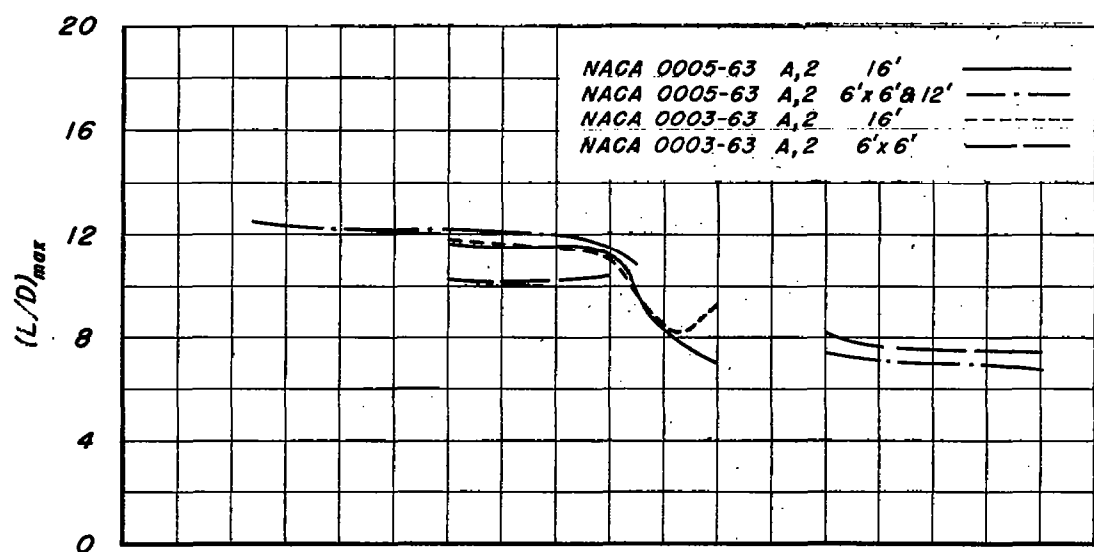
(b) C_D vs M

Figure 9.—Continued.



(c) $\frac{dC_m}{dC_L}$ vs M

Figure 9.-Continued.



(d) $(L/D)_{max}$ vs M

Figure 9.-Continued.

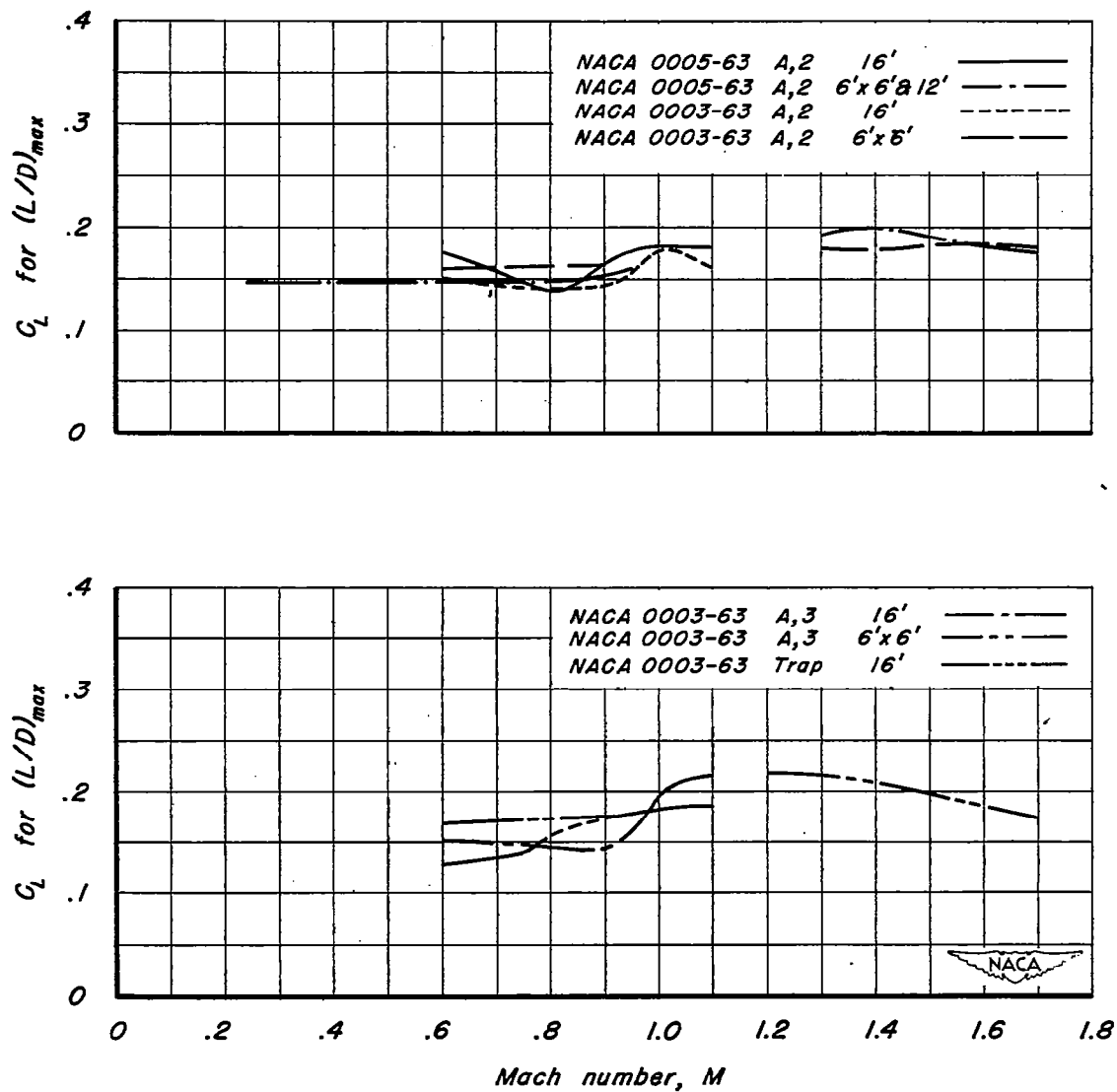
(e) C_L for $(L/D)_{max}$ vs M

Figure 9.-Concluded.

SECURITY INFORMATION

[REDACTED]



NASA Technical Library

3 1176 01434 8222



[REDACTED]